5-22-2006

Behavior and Flexure Analysis of Balsa Wood Core Sandwich Composites: Experimental, Analytical and Finite Element Approaches

Sandeep Nallagula
University of New Orleans

BEHAVIOR AND FLEXURE ANALYSIS OF BALSA WOOD CORE SANDWICH COMPOSITES: EXPERIMENTAL, ANALYTICAL AND FINITE ELEMENT APPROACHES

A Thesis

Submitted to the Faculty of the
University of New Orleans
in partial fulfillment of the
requirements for the degree of

Master of Science
in
Engineering

by

Sandeep K Nallagula
B.S. J.N.T. University, 2003
May 2006

Acknowledgement

I take this opportunity to thank my principal advisor, Dr. David Hui, for his constant encouragement, his valuable suggestions on experimental approach and his ways of verifying the authenticity of the experimental data with basic principles of engineering. I would also like to thank my co-advisor, Dr. Richard P Donovan, for his patience, valuable suggestions and for introducing me to the field of Finite Element Analysis, Dr. Piyush K Dutta for supplying the test coupons and advising me to try new techniques, Dr. Leo Daniel for supervising my work and suggesting that I follow the right direction and Dr. Paul Herrington, chair, department of Mechanical Engineering and Dr. Carsie Hall, associate professor, Mechanical Engineering for being a part of my thesis committee.

My special thanks to Ms. Gloria Carter at Montana Tech of The University of Montana, the engineering staff at the University of New Orleans, Mr. Daniel Samborsky at Montana State University, who introduced me to the experimental field and helped me to learn many basic principles of engineering, and testing on the MTS machine. Special thanks to Dr. Richard Donovan and Ms. Gloria Carter for their constant encouragement and patience. I also would like to thank the US Army for supplying the test coupons and Montana State University for providing me an opportunity to work on the MTS machine.

Finally I would like to thank my family and friends for their constant support and help in dealing with difficult times, my heartfelt thanks to my dad, Mr. Srawan Nallagula, who is a constant source of inspiration in my life, and also for his extended support throughout my career.

This work was partially sponsored by the office of Naval Research to the University of New Orleans and was monitored by Dr. Yapa D.S. Rajapakse.

Table of Contents

List of Figures

List of Tables

List of Appendices

Abstract

The load-deflection behavior of a US Army Corps of Engineers available sandwich plates in three-point bending with glass phenolic facings and balsa wood core is being investigated under room and elevated temperatures. Test data on bending rigidity, critical interfacial failure (skin-to-core interface) and shear stress are collected and analyzed. The load-deflection curves plots up to the point of failure initiation are being studied. The effects of the span and the radius of the loading nose on the bending modulus and strength are examined systematically. Theoretical calculations from a modified beam theory of sandwich structure are applied and the effect of the shearing rigidity of the core is studied, and the propensity with respect to the span is also investigated. A finite element model is developed to study the flexural and stress analysis. Based on the results, this thesis proposes a desirable analytical approach that correlates theory with experiment as defined below.

Chapter 1: Introduction

1.1 Composite Materials

Most materials used in engineering structures are combinations of distinctly different materials. However, because there is no clear micro-structure to distinguish the individual constituents, these materials are idealized as monolithic materials. Material properties are fundamentally average quantities obtained from tests on bulk materials.

Composite materials are differentiated by the existence of a clearly identifiable microstructure. Some traditional materials such as reinforced concrete and wood fall in to the broad category of composite materials. For the purpose of discussion, composite materials are presumed to consist of a matrix (typically isotropic) such as epoxy or polyester and one or more reinforcing phases (also typically isotropic). The reinforcing phases are further classified as particulate, discontinuous fiber or continuous fiber. The figure 1 illustrates loading and stacking sequence of the plies for manufacturing a laminate plate.

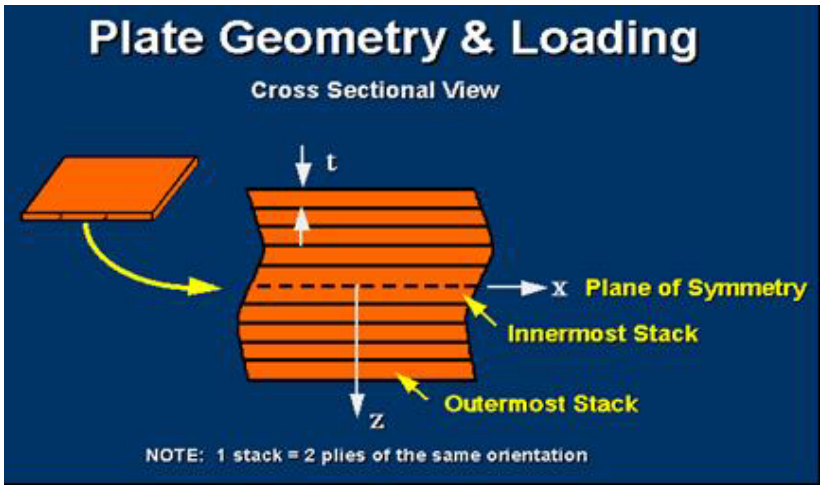

Figure 1: Plate geometry and loading [14]

By carefully selecting the materials and carefully controlling the process, these constituents can be combined to form a composite material tailored to a specific application. This utility is tempered by increased complexity due to the anisotropy of most composite materials.

Composite materials are becoming prevalent in many industries like aerospace, sporting goods and the construction industry. Aerospace industry takes maximum advantage of composite materials i.e. aerospace industry uses more composite materials when compared to any other industry. Figure 2 shows different materials used in manufacturing of an airplane.

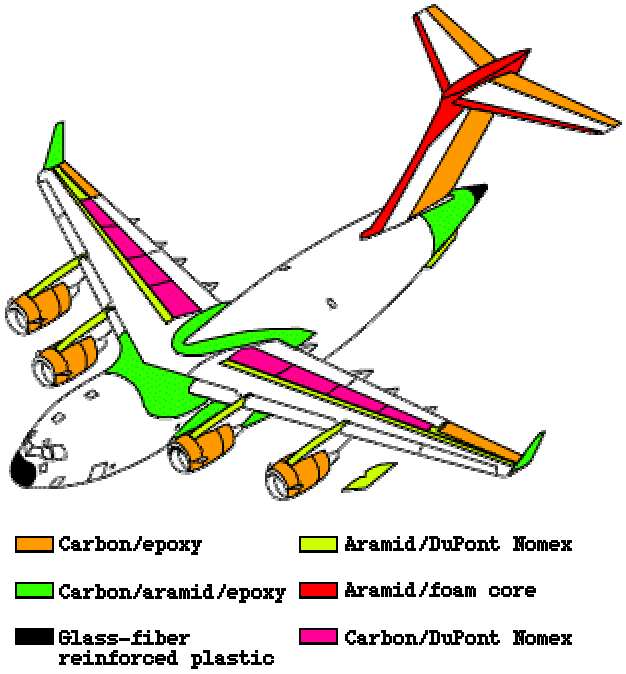

Figure2: Materials used in manufacturing of an airplane [14]

1.2 Sandwich Composites

The following is the sandwich structure concept described by the American Society of Testing and Materials.

A Structural Sandwich is a special form of composite comprising of a combination of different materials that are bonded to each other so as to utilize the properties of each separate component to the structural advantage of the whole assembly.

In order to utilize the material properties to the maximum, the normal sandwich composite consists of a core between the two thin layers called the facing sheets. The core is glued to the two facings forming two additional glued sides in a complete sandwich composite. This type of composite has a type of stressed-skin construction in which the facings resist nearly all of the applied edgewise (in-plane) loads and flat-wise bending moments. The core provides the necessary shear strength to the structure. By making the correct choice of the facing materials and core, high strength to weight and stiffness to weight ratios can be achieved using this structure. The facing sheets are strong and under perfect bonding conditions, form a perfect sandwich composite material. The basic design concept is to have strong, thin facings far enough apart to get good stiffness to weight ratios and a light weight core that can handle the shear and can stabilize the two facings attached to it through a strong bonding medium. The sandwich composite can be compared to an I-beam, which can be regarded as optimized with regard to the cross sectional geometry. However, in the I-beam and in the sandwich composite, most of the normal stresses will be carried through out by flanges or faces and the shear stresses by the web or the core in the sandwich respectively. In addition to these, the core should provide sufficient stiffness to avoid local buckling. Figure 3 below shows the Simple I-beam and an infinite I-beam which is comparable to a sandwich panel. [16]

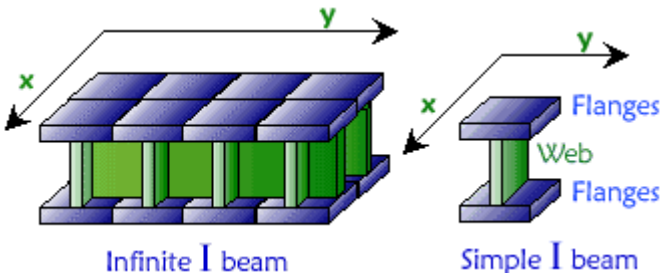

Figure3: Simple I-beam and a sandwich [16]

Sandwich materials can be classified based on the type of facing sheets and also the type of core used. Based on the core type classification of sandwich materials, we have foam-type core sandwich composites, honeycomb core sandwich composites and corrugated core sandwiches. The honeycomb core is usually manufactured from an aluminum foil. The ordinary honeycomb tends to bend anti-clastically and might not fit in a given shape but improved version of it is available, which has a flexible core and can provide good formability. Facing sheets can be made from aluminum, stainless steel or other alloys. Some facings like hardboard, plywood, glass reinforced cement, plaster board and resin impregnated paper etc are being used for construction purposes. These are also called fiber-reinforced laminates. Depending on the use of the sandwich composite and the application, different cores can be glued to different facings. The major flexibility is that almost any core can be glued to any facing sheets. Figure 4 illustrates the facings and the core being glued to form a sandwich panel. The top part of the figure shows stacked and bonded fiber-reinforced sheets.

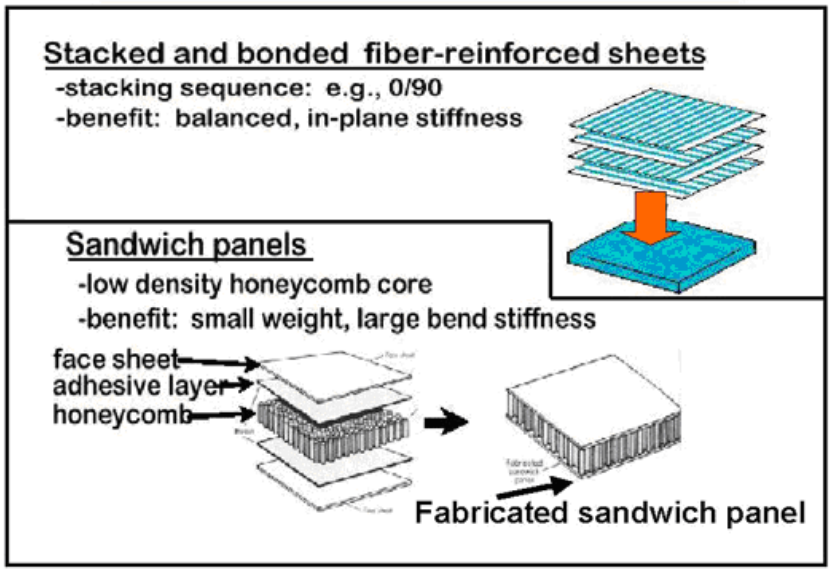

Figure4: Structural composites [14]

When edge wise loads are applied on a sandwich composite, it results in four different types of failure modes as illustrated in figure 5.

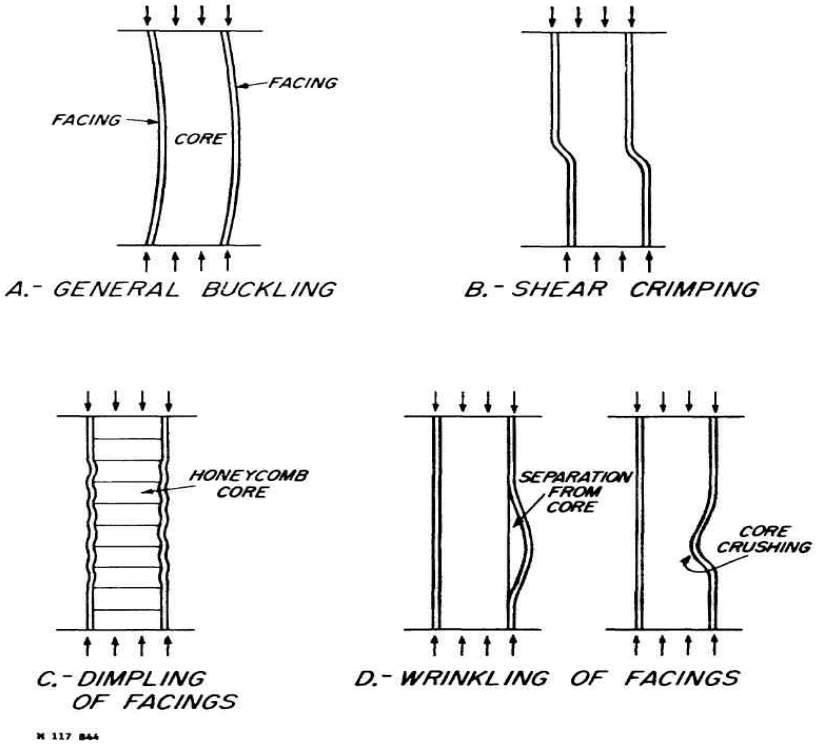

Figure5: Failure Modes when edge wise loads are applied [14]

The likelihood of initiating one of these failure modes can be reduced by following some basic design principles [15]. The selected core should be thick enough to handle the shear stresses. It should have enough shear rigidity to avoid local buckling, the sandwich facings should be at-least thick enough to handle the stresses at the design loads, the sandwich core should possess enough modulus of elasticity to keep itself strong and for a honeycomb or a corrugated core, the corrugation spacing or the cell size should be small to avoid failure.

Almost any structural material with thin sheets can be used as facings for the sandwich composite panel. As of today, we have a large number of facings available in the market for sandwich construction, making it possible to manufacture a sandwich composite according to its actual demand. The facings can be classified into two groups; metallic facings and non- metallic facings

Some examples of metallic facings are titanium, aluminum, and stainless steel. Some of non-metallic facings which are commonly used include fiber reinforced plastics (FRP's) like glass fiber reinforced plastic- GFRP, carbon fiber reinforced plastic- CFRP, and Kevlar fibers with different resins like phenolic, polyester and epoxy.

The primary demands on facing materials are high tensile and compressive strength, good surface finish, good impact resistance, good water resistance, good environmental resistance, and high stiffness and high flexural rigidity.

The core is an important element of a sandwich composite. Honeycomb cores are used in the aeronautical industry. Unfortunately, the honeycombs are expensive and cannot resist high impact loads which limit their application to relatively protected structures. The corrugated cores

are used in ship building and packaging industry. The cellular cores like the balsa wood core provide a nice core quality within a good price and are therefore used in maritime structures. They can operate in tough environments compared to honeycomb or corrugated cores. Some examples of honeycomb materials are aluminum, glass fabric, asbestos fabric, plastic film, paper, steel, heat resistant alloy and titanium. Examples of materials used in making corrugated core are glass fabric and steel. Some examples of materials used for making foam cores are foamed plastic, foamed glass, foamed aluminum, and balsa wood, which is considered a natural foam type core.

To permit an airframe sandwich construction to perform satisfactorily, the core of the sandwich must have certain mechanical properties and thermal characteristics under conditions of use and still conform to weight limitations. Sandwich cores of densities ranging from 1. 6 to 23 pounds per cubic foot have found use in airframe sandwich, but the usual density range is 3 to 10 pounds per cubic foot.

Figure 6(a) shows a sandwich composite consisting of a foam type core. Figure 6(b) shows a honeycomb core, Figure 6(c) shows a unidirectional corrugated core, Figure 6(d) shows variation of the unidirectional corrugated core with back to back corrugation

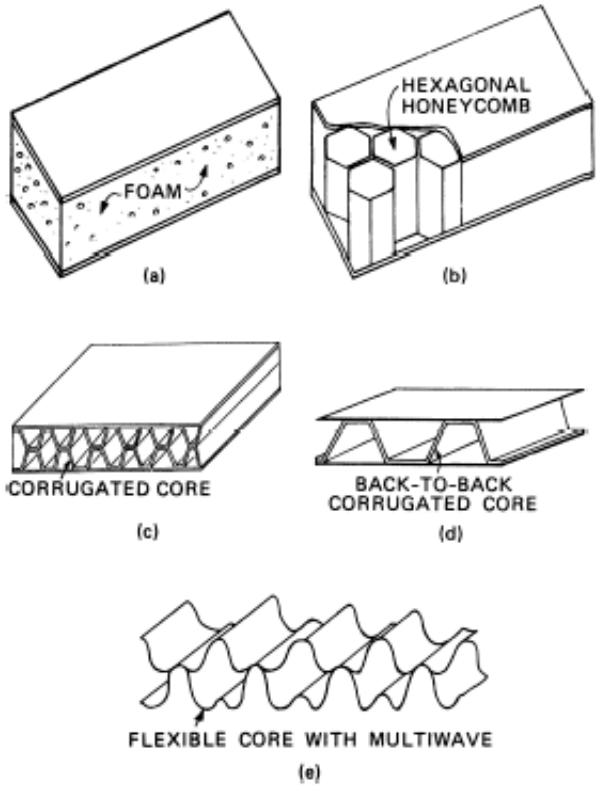

Figure6: Types of core materials in sandwich composites (a) foam, (b) honeycomb, (c) corrugated, (d) back to back corrugated and (e) flexible core [12]

The demands of the core materials require that they should have sufficient thermal insulation, low density, sufficient thickness, sufficient shear stiffness, sufficient stiffness to prevent local buckling, and sufficient shear strength to prevent core shear failure. Also the core should be hard enough to bond the facing sheets to it and must provide enough shear strength to the facing sheets so that they don't move relatively apart. The facings should be stiff enough to protect the sandwich from buckling upon compression or tension.

The mathematical equations characterizing the sandwich composites are more difficult than material with just a single layer involved. They contain larger number of higher order

differential equations containing more variables and are often coupled. Approximate solutions may be necessary for most of the practical problems in this field.

1.3 Applications of Sandwich Composites

1.3.1 Aeronautical Applications

Some of the first aeronautical structures to take advantage of the sandwich panel construction were the Comet Racer, Albatross Passenger and the De Havilland Mosquito illustrated in Figure 7. These planes proved to the world that lighter and superior aerodynamically shaped streamlined aircraft can be achieved compared to the similar aircraft made of metal. The Mosquito possessed a superior performance in terms of speed and agility which made it a good aircraft for the military use.

Figure7: De Havilland Mosquito, the first mass produced (1940-1950) sandwich structure [14]

In the early 1980's composite sandwich structures became more prevalent in both civilian and military aircrafts. Mass produced civilian aircrafts like the Airbus A300 only included about 1% composite parts but the newer civilian aircrafts like Airbus A 340 and A380 include 13% and 25% composite parts respectively. Figure 8 illustrates the development of Airbus airplanes over the years. Military aviation applications are ahead of civilian aviation but similar development is being seen here. The General Dynamics F-16, developed in the late 1970's used just 3% of composite parts while the newer fighter/bomber, Lockheed/Boeing F-22, developed in the early 1990's uses 23% composite parts.

During the last few years, the concept of the sandwich structures has entered into the business jet manufacturing industry. These small jets, able to seat six to twelve passengers, travel across the ocean without refueling at a speed comparable to the large commercial jets. Such airplanes can bring corporation executives from one part of the world to another in a time saving fashion. Without the application of sandwich composites, this would not have been possible for the aviation industry.

Figure8: Development of Airbus airplanes over time [14]

1.3.2 Maritime Applications

The sandwich structures have been used in maritime applications since the middle of the last century. In the beginning, sandwich composites were used to build pleasure boats but now they are also used in high performance power boats. The initiative to build larger vessels came just as aeronautical industry was taken over by the military. Initially, single skin composites were used in the BRITISH Hunt and the SANDOWN mine hunter classes. The British Hunt and SANDOWN mine hunter classes are illustrated in the Figures 9 and 10 respectively. The development of a sandwich with PVC foam and fiber composite proved to be highly efficient, economical, and low weight for large vessels made for large vessels that were lighter in weight. For example, mine counter- measure vessels, which were made of wood demanding high maintenance costs, can now be made of sandwich composites.

Figure9: The British Hunt [14]

Figure10: The SANDOWN mine hunter [14]

The fiber reinforced plastics (FRPs) sandwich construction has also been widely used in the recent past for small to medium sized boats, military as well as civilian boats like the Minesweeper and ferry boats which are popular in Australia and Scandinavia. The concept of using a thick sandwich composite hull has been noticed in the recent years. They can provide certain advantages over the conventional ship building materials.

Figure11: The British Mirabella [14]

1.3.3 Construction and Infrastructure Applications

Due to the price drop of the FRP unit, the momentum of construction and infrastructure industry has picked up in the recent time. FRPs have advantages over metals such as corrosion resistance and free from magnetic effects. Large scale applications are being expanded into building construction and highway bridges. They include not only new constructions, but some rehabilitation projects.

The above examples are only from aerospace, maritime and construction projects but the concept of sandwich composites plays an active role in areas like in the energy industry, for building wind generator blades. Sandwich composites are also used in train and automotive industry to manufacture parts like bonnets, crash beams and secondary parts in automobiles. Apart from all these, they are also used in the packaging industry.

Chapter 2: Literature Survey

2.1 Thermal Effects on Sandwich Composite

Sandwich composites are used in shipboard structures, aerospace engineering, vehicle construction, cargo packing etc. The main concern for using sandwich composites in shipboard structures is fire. Before the sandwich composite even reaches the ignition temperature, the structural integrity of the sandwich composite is degraded. Dr. Hui and Dr. Dutta [1] worked on the fire aspect of sandwich composites. They understood and predicted the survival time available before the structure actually collapses completely. They worked on predicting time for failure of thick composite structures under fire and a non-uniform fire development on both the sides. An experimental study of balsa wood core composite sandwich (BWCCS) at different temperatures under a flexural load was done. Two experiments were done the first being studying the temperature distribution along the thickness of balsa wood core composite sandwich and the second being studying a three-point bend test at two different temperatures one at 20 degrees centigrade and the other at 79 degrees centigrade.

The balsa wood core composite material was hot pressed with Fiber Reinforced Polymer 1208(FRP-0, 90) skin. The dimensions of the balsa wood core composite material were 12ft x 6 ft. Thicknesses of ¾ in and 1 in were studied upon. The properties of the FRP skin material were determined. The test coupon they used was a dog bone shaped skin which was prepared by taking the balsa wood core out of the sandwich composite panels and by cutting the skin into a dog bone shaped coupon. Three such coupons were prepared and were tested by performing a

tension test on a MTS Universal Testing Machine. An extensometer was used to calculate the strain and the feed rate given was 0.05 in/min. The Figure 12 shows the skin tension test.

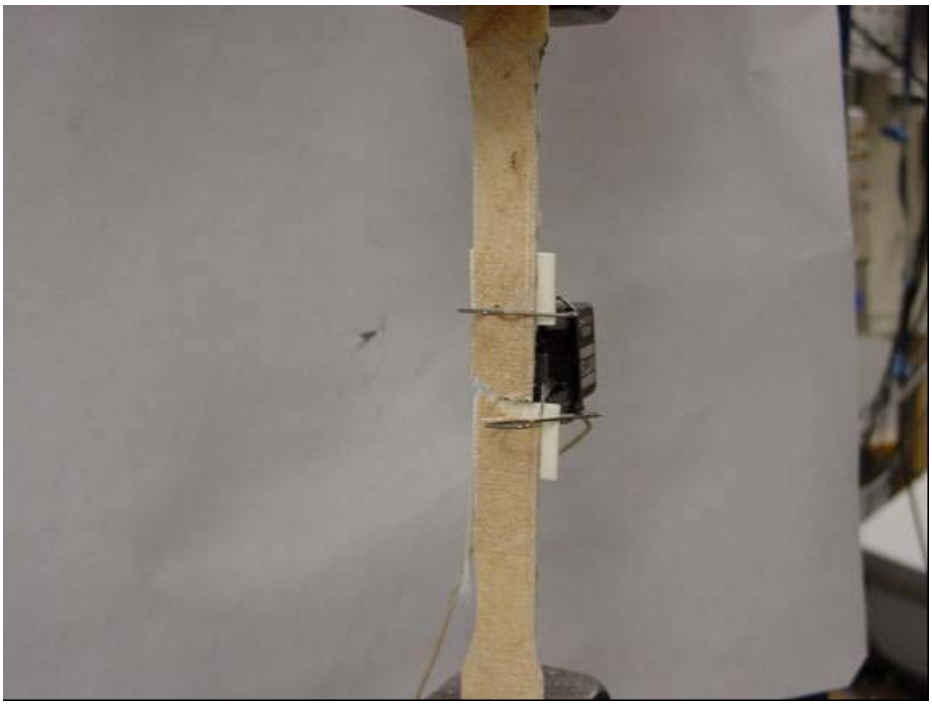

Figure 12: Skin tension test in the moment of breakage [1]

The time taken for the skin to fail was 4 to 5 minutes. The results of these tests were tabulated and summarized from which it was said that the modulus of skin was 1,140,000 psi. Typical Stress- Strain curves were also drawn.

Figure 13 illustrates the actual dimensions of the sandwich coupon along with the span length used in three-point bending.

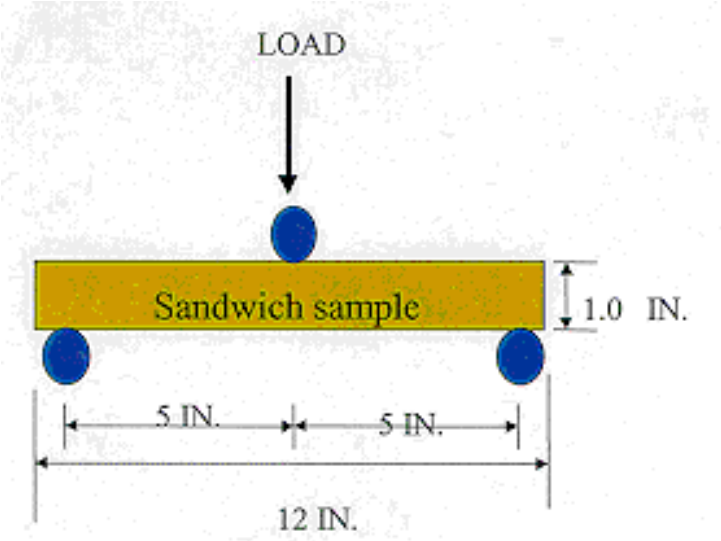

Figure 13: Dimensions of sandwich composite used for testing [1]

The three-point bend test was also performed according to the ASTM C 393 standard to measure the temperature gradient and to establish temperature regimes on both the sides of a sandwich composite. The results were used to predict the time taken to reach a temperature of 80 degrees centigrade in three-point bending. It took 30 minutes to step up the temperature in the chamber from 20 degrees to 79 degrees centigrade. This test was performed on an MTS machine and the loading fittings were arranged according to the ASTM C 393 standard at two different temperatures, one at 20 deg centigrade and the other at 79 deg centigrade. The span length used in the experiment was 10 inches when the sandwich length was 12 inches. The load was applied to the specimen at a constant rate of 0.05 in/min and the maximum applied load occurred at about 5- 6 minutes. The load and displacement data were recorded.

Figure 14 illustrates the skin failure under an application of a load in three-point bending.

Figure 14: Skin failure [1]

Using these results, they found that both the skin test and three-point bending test show that both the skin and the sandwich composite fail in a brittle manner. They also noticed that the sandwich core has an insulating effect. They said the temperature gradient is steeper in a thinner sandwich material and the reduction of strength is 12% for the thick and 10% for the thin sandwich structures.

2.2 Collapse of Sandwich Structures in Three-Point Bending

V.L Tagarielli et al.[2] studied collapse of clamped and simply supported composite sandwich beams in three-point bending. The composite sandwich beams consisted of glass-vinylester face sheets and a PVC foam core. These composites are tested by three-point bending test under a quasi-static load. The study focused on simply supported and clamped boundary

conditions in three-point bending. Analytical formulae were developed for parameters like elastic stiffness and initial collapse strength of composite beams. Post yield response is modeled using a membrane assumption. Clamped and simply supported sandwich beams comprised of PVC foam core and woven glass face sheets were tested in three-point bending and their load vs. deflection response contrasted. Experimental results are compared with finite element predictions. In analytic modeling for stiffness of sandwich beams, simple formulae for stiffness and collapse strength of simply supported and clamped sandwich beams were summarized.

2.3 Analytical formulae for stiffness of sandwich beams

The elastic deflection δ is the sum of flexural and shear deflections and for simply supported beams,

$$\delta = \frac{Pl^3}{48EI_{eq}} + \frac{Pl}{4AG_{eq}} \tag{2.1}$$

Where

$$EI_{eq} = \frac{E_f btd^2}{2} + \frac{E_f bt^3}{6} + \frac{E_c bc^3}{12} \approx \frac{E_f btd^2}{2} \tag{2.2}$$

and

$$AG_{eq} = \frac{bd^2}{c} G_c \approx bcG_c \tag{2.3}$$

Here E_c, G_c are Young's modulus and shear modulus respectively, of the core material and d= c + t and for the clamped beams, elastic deflection is given by

$$\delta = \frac{Pl^3}{384EI_{eq}} + \frac{Pl}{4AG_{eq}} \tag{2.4}$$

The critical loads for fiber micro-buckling, core shear and indentation for simply supported beams are given in equations 2.5, 2.6 and 2.7

$$P_{fm}^{ss} = \frac{4dbt\sigma_f}{l} \tag{2.5}$$

The superscript 'ss' refers to simply supported, while the subscript 'fm' refers to face micro buckling.

$$P_{cs}^{ss} = 2bd\tau_c \tag{2.6}$$

Where τ_c is uniform shear strength.

$$P_{in}^{ss} = bt\left(\frac{\Pi^2 dE_f\sigma_c^2}{3l}\right)^{1/3} \tag{2.7}$$

The critical loads for fiber micro-buckling and core shear collapse are given in equations 2.8 and 2.9.

$$P_{fm}^{c1} = \frac{8bdt}{l}\sigma_f \tag{2.8}$$

$$P_{cs}^{c1} = P_{cc}^{ss} = 2bd\tau_c \tag{2.9}$$

They also analyzed large deflection of clamped beams. This study explores the effect of simply supported and clamped boundary conditions upon the load versus deflection response of composite sandwich beams. The above formulae were derived and experimentally verified.

Judawisastra et al. studied a relatively new material which is based on woven sandwich fabric platform [3]. The core shear properties of this kind of material were investigated by two methods: three-point bending test and a shear test. This new type of material has been used in many applications like hardtops for cars, side spoilers for trucks, radar domes, mobile homes, small aircrafts, train fronts, polyester boats, furniture and interior wall panels for fast ferries. This material provides a delamination resistant sandwich since the top and bottom of the skin are interconnected by pile yarns. The skin is made of glass carbon fibers and impregnated with epoxy, phenolic, or other thermoset resins. The core can be foamed up with liquid foam injection. The focus was on evaluating the shear properties of three dimensional woven sandwich fabric panels. There could be problems in this case because of the vertical orientation of the pile yarns, especially for long vertical pile yarns as illustrated in the figure 15.

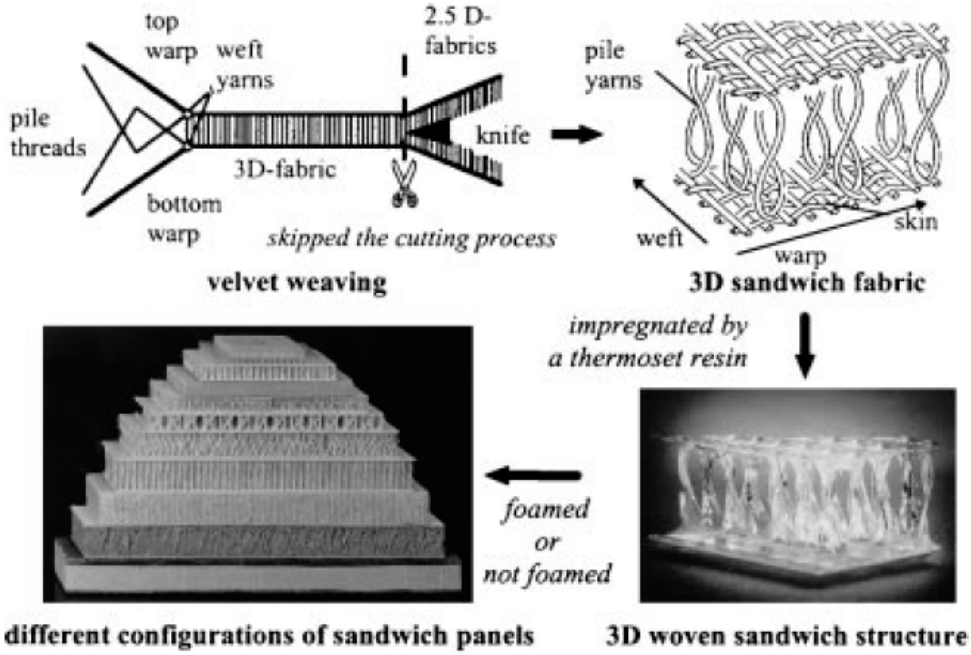

Figure 15: Vertically oriented pile yarns and the expected shear due to the vertical orientation of the pile fibers [3]

Figure 16 illustrates the importance of sufficient stiffness of these panels. It compares the flexural behavior of an un-foamed panel with high pile length and foamed panel with short pile length. Figure 16(a) shows the bending of the sandwich beam in which deflection is caused by core shear which means that the sandwich effect of using two separate skins is lost at short span lengths and there is a large risk of core failure at low loads. Figure 16(b) shows normal bending at same span length.

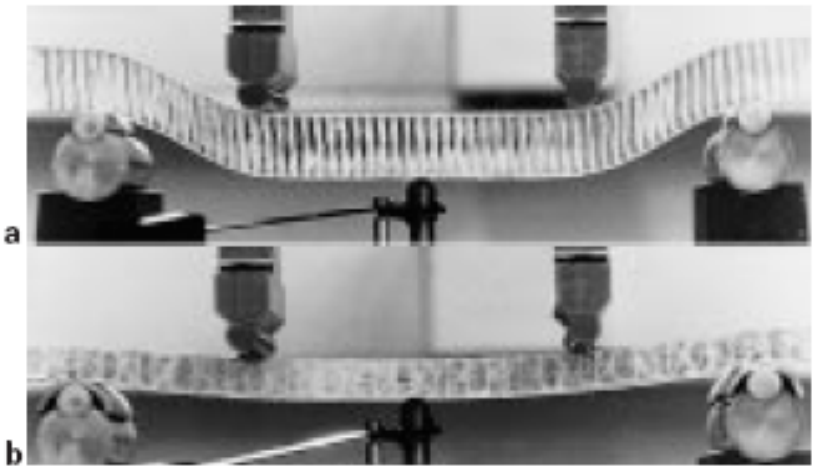

Figure 16: (a) and (b) Stiffness of the panels [3]

2.4 Evaluation of core shear properties

Judawisastra et al. evaluated the core shear properties like core shear modulus and strength of four types of three dimensional woven sandwich panels. Three-point bending test and shear tests were conducted for examining and determining the properties. They proposed the following formulae for a three-point bend test with a vertical deflection of 'w' under the central load 'P'.

$$w = \frac{Pl^3}{48D} + \frac{Pl}{4N} \tag{2.10}$$

For sandwich beams, the flexural stiffness ignoring the contribution of core is given in equation (2.11) and the sandwich shear stiffness N is given by equation (2.12)

$$D = \frac{E_s \left(h^3 - c^3\right) b}{12\left(1 - \upsilon^2\right)} \tag{2.11}$$

$$N = \frac{G\left(h + c\right)^2 b}{4c} \tag{2.12}$$

The core shear failure will occur at shorter span lengths in a three-point bend test. The core shear strength, τ_{cr} can be calculated as

$$\tau_{cr} = \frac{P_u}{\left(h + c\right) b} \tag{2.13}$$

They also conducted shear test in which the line of load is slightly tilted with respect to the specimen mid-plane so that the line of load application is in the sandwich mid-plane. Figure 17 illustrates the setup for the shear test.

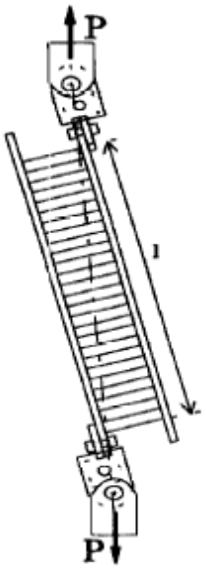

Figure 17: Shear test set up [3]

The core shear strength τ_{cr} was also be determined by a shear test. The equation is as follows:

$$\tau_{cr} = \frac{P_u}{b \times l} \tag{2.14}$$

Finally, they derived a formula to calculate the effective shear modulus of sandwich specimen G.

$$G = \frac{P}{bl} \times \frac{h}{s} \tag{2.15}$$

Flexural tests have a few advantages over the conventional tests. They are simple to perform and the core shear properties and in-plane properties of the skin can be evaluated at the same time.

Judawisastra et al. are investigating to check whether the shear properties can be brought to an acceptable level by weaving some of the piles below 45 degrees, by using sufficient resin content or by adjusting the degree of stretching.

2.5 Three-Point test modes

In 1971, Ogorkiewicz et al. conducted three-point bend tests with six different modes of supporting the specimen. The testing was done on fiber-plastics. Bending tests involve a number of variables which can significantly affect the results and therefore need to be carefully considered when they are used to determine the mechanical properties of fiber-plastic composite materials. Ogorkiewicz et al. proposed that there is a further need for a systematic analysis of variables involved in three-point bending even after it was done numerous times before. They have examined a number of different methods of supporting the specimens and in each case they correlated the corresponding load and deflection values which took in to account the specimen material and the support system. They conducted three-point bending tests using a number of different support systems like knife edge supports, large radius supports, medium radius supports, large diameter, rotating roller supports, rotating rollers on swinging links and small diameter roller supports. A discussion of each support system follows.

2.5.1 Knife edge supports

Knife edge supports are used quite often in a three-point bend test. In theory, they give a line contact between the supports and the specimen. In general, knife edge supports are designed

with fixed radii based on the requirements at a particular material system to which case, they were milled at right angles of two surfaces from a steel block which gave them a nose radius of 0.063 mm.

2.5.2 Large radius supports

The primary disadvantage of knife edge supports is that they might cause local indentation on the specimen upon application of normal load. A large indentation can affect the deflection of the specimen. The procedure or practice used to minimize indentations is by using supports of large radii. A radius of l2.7 mm for semi steel cylinders was used in this case.

2.5.3 Medium radius supports

Large radius supports suffer in turn from the disadvantage that the point of contact between them and the specimen varies with the deflections. There is a strong case therefore for considering a compromise between the knife-edges and the large radius rollers, which in this case, means steel semi-cylinders with a radius of 6.8mm.

2.5.4 Large Diameter, rotating roller supports

The fixed supports were replaced by large rollers mounted on ball bearings. This method seemed to minimize the effect of friction at the supports and to make the rotating rollers directly comparable with the fixed supports because they had the same 12.7 mm radius.

Figure 18 illustrates six different types of supports used in three-point bending: knife edge supports, large diameter fixed supports, medium diameter fixed supports, large diameter roller supports, large diameter roller on swinging links, and small diameter roller supports.

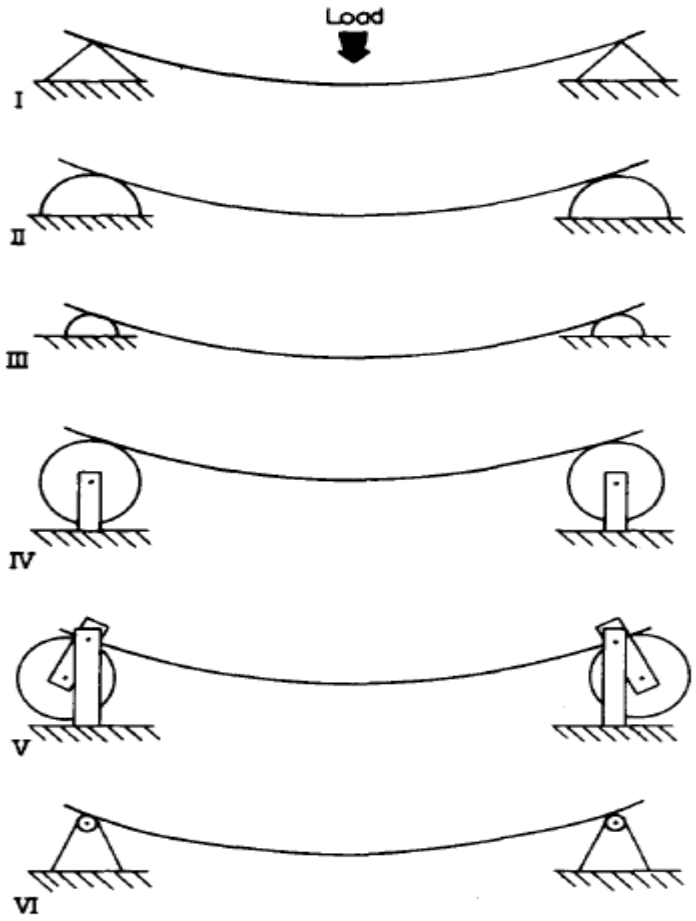

Figure 18: Six different types of supports used in three-point bending

2.5.5 Rotating rollers on swinging links

The next refinement to large diameter rotating roller supports which was developed by Swanson to test metals. He mounted the bearings on the links which pivot on an axis parallel to the roller axis and displaced from it by a distance equal to the radius of the roller. Compared to the other type of supports, the span is constant in this case. This case also retains special

advantages like large diameter, rotting roller supports. The rollers had a 12.7 mm diameter and the links were mounted on the bearings.

2.5.6 Small diameter roller supports

This system has small rollers which rest in semi circular grooves machined into blocks of steel. This method of support approximated the knife edge type but offered the potential advantage of lower contact stresses and the choice of having the roller free to rotate or be fixed. In the latter case, it was equivalent to knife edge supports with large nose radii but the rollers made the radius easier to define and to achieve to a high standard of surface finish. The rollers were made of 3.5 mm diameter ground silver steel rod and were fixed or made free to rotate by the use of grooves giving tight and slack fits, respectively.

Even smaller, 2.4mm diameter rollers were considered and were adjudged to be the smallest that could be used, if they were to be adequately stiff and true and thus give uniform contact across the width of the specimens.

2.5.7 Evaluation and examination of specimens

Two materials, steel and permaglass, were used to evaluate the testing fixtures. The specimen dimensions are given in table 1.

Table 1: Dimensions of the specimen used

Specimen material	Length (mm)	Span (mm)	Thickness (mm)	Width (mm)	Span to thick-ness ratio	Widthto thick-ness ratio
Steel	228	200	0·813	13·46	250	16·5
Permaglass	292	200	3·175	18·28	64	5·8

The span-thickness and width-thickness ratios were well above the ASTM standards. Possible effects of transverse or anticlastic curvature were neglected because of the value of

$$b = \frac{(width)^2}{thickness \times radius\ of\ curvature}$$

The supports were bolted on to the ground surface of a leveled and welded frame. The centers of the specimen in each case were in the middle of the support span and their deflection was recorded by means of a dial gage. Sometimes, the deflection was also recorded by a cathetometer but it was not very accurate. A light saddle with a knife edge was used to apply loads on the specimen at mid-span. Weights were placed on the pan which was connected by a loosely fitted rod so its weight could be balanced. The pan was supported by a hydraulic jack, which when released, enabled the load to be applied on the specimen at a constant rate. Even though permaglass behaves virtually linear elastic, specimens were tested by applying a series of progressively increasing loads and unloading after each load for a total of four tests. The steel specimens were loaded by simply adding weights to the pan. Deflection was recorded 100 seconds after it was loaded. Load- deflection curves for the steel specimens were time independent.

Ogorkiewicz et al. tested at least four specimens of each material, each of which was tested twice. Experimental results obtained with different supports are summarized in the Figures 19 and 20.

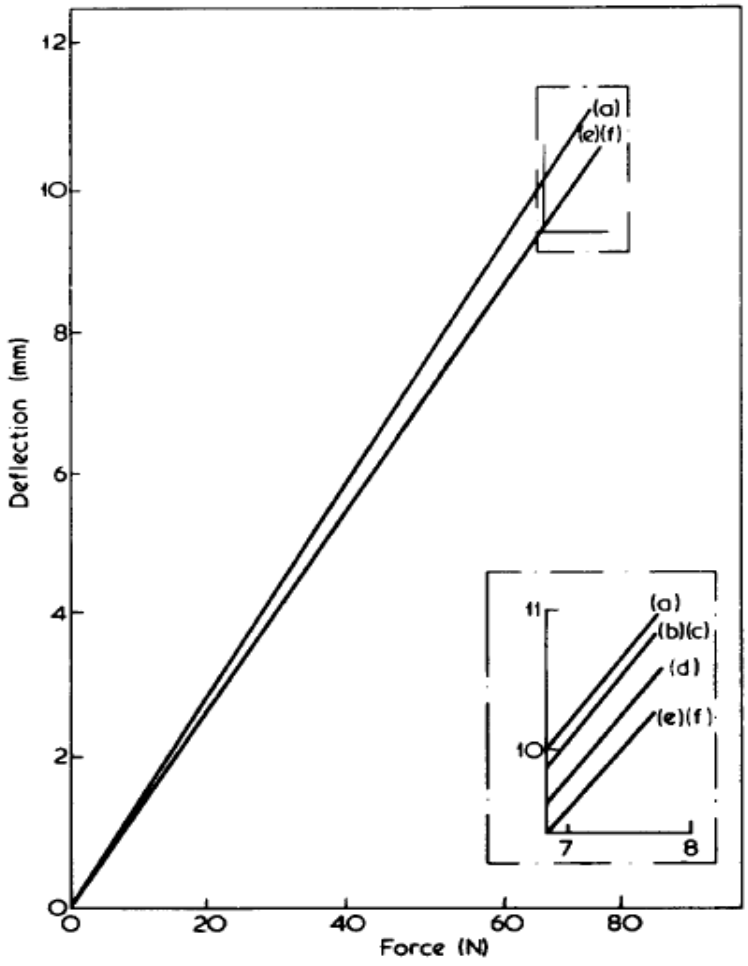

Figure 19: Experimental load-deflection curves for steel specimens on different supports

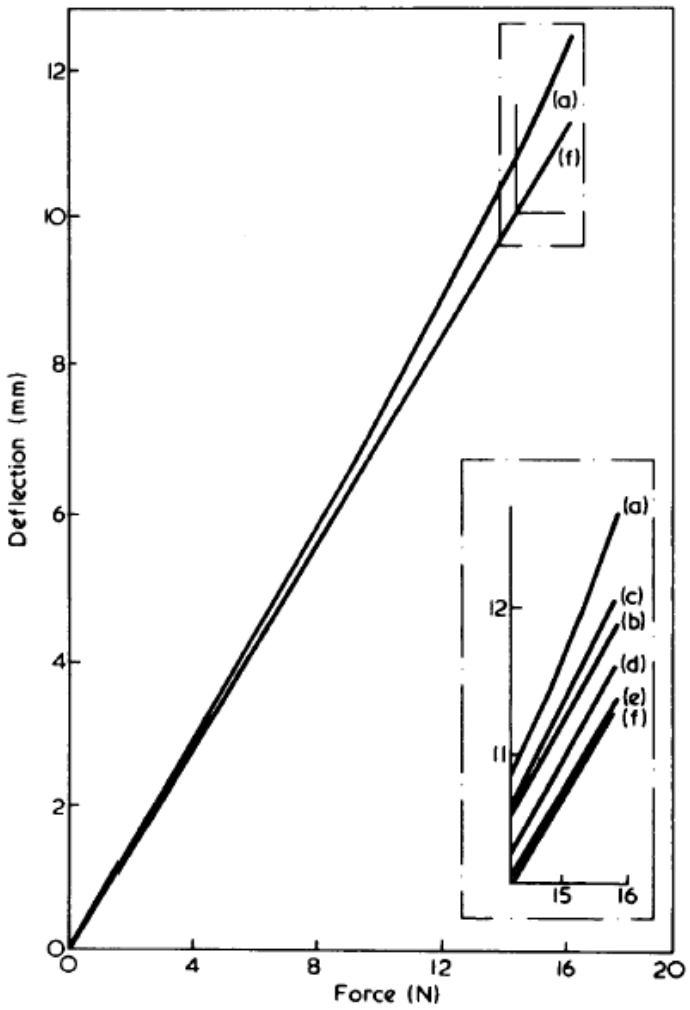

Figure 20: Observed and calculated deflections of steel and permaglass specimens on knife-edge supports [4]

2.6 Analysis of different kinds of Supports

The knife edge supports were the simplest to analyze. The following is the deflection equation when the deflections are small and the materials of the specimen are linearly elastic.

$$\delta = \frac{w l^3}{48 E I}$$

(2.16)

Where W= load

L= span

E= modulus of elasticity

I= second moment of area of cross section.

When the above equation is applied to steel specimen, the calculated deflections coincided with observed deflections only when they were small. When the deflections increase, the above equation becomes invalid and the deflections calculated continue to increase linearly with the load. To obtain more realistic values of deflection, Freeman's solution was used [4].

$$\delta = \frac{wl^3}{48EI} \frac{\cos\alpha \times Q^3(\alpha)}{6S(\alpha)} \qquad (2.17)$$

Where $Q(\alpha)$ and $S(\alpha)$ are the functions of the angle α which the beam makes with the horizontal at the supports.

A large number of variables need to be considered for testing of plastics in three-point bending. A judicious choice can reduce the number of extraneous variables and make it simpler and more attractive in terms of the analysis of deformational study of plastics. The most appropriate choice is to use long slender specimens supported on small diameter rollers located in semi circular grooves.

2.7 Static and dynamic three-point bending of Sandwich Composites

In 2005, V. Crupi and R. Montanini studied three-point bend tests for aluminum foam sandwiches under static and dynamic loading. They conducted three-point bend tests to investigate the structural response, i.e. collapse modes, energy dissipation and strain rate sensitivity of two different types of aluminum foam sandwich panels consisting of a closed cell aluminum foam core with two integral (Schunk) or two glued (Alulight) faces.

Aluminum foam sandwiches obtained by combining metal face sheets with lightweight metal foam have peculiar properties such as low specific weight, good energy dissipation, high impact strength, acoustical insulation, thermal insulation and high damping. They have an edge over the traditional honeycombs as they can be curved into different shapes with integral skins, allowing higher working temperature and higher resistance to damage from water intrusion.

Two different aluminum alloys, consisting of AlSi7 foam core and AlMn1 faces and the other consisting of AlSi10 core and Al (99.5%) faces were examined. Preliminary analyses such as examination of the microstructure and chemical composition of both types of aluminum foam sandwiches were done following lapping process. Small quantities of titanium were found in both the typologies due to Ti hydroxide used as foaming agents in the manufacturing process. See figure 21.

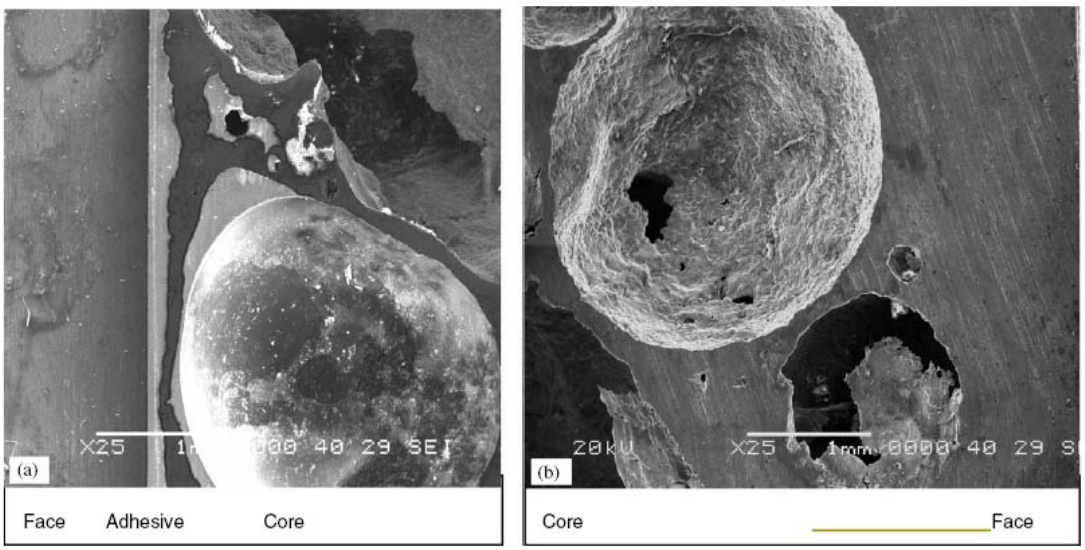

Figure 21: SEM micrograph of the core-skin interface [5]

Three-point bending tests were done on a Universal Testing Machine using a 10KN load cell as illustrated in Figure 22. The feed given to the piston was 2mm/min with a preload of 10N. Dynamic three-point bending tests with an initial velocity up to about 1.2 m/sec were performed using an instrumented pendulum machine as illustrated in Figure 23.

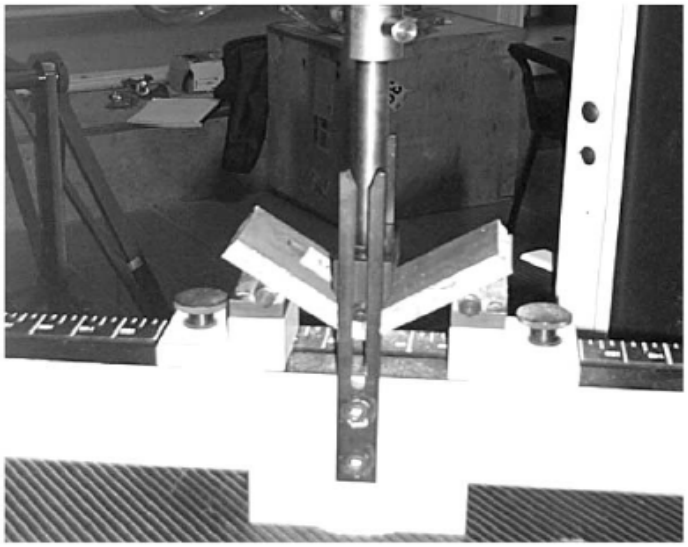

Figure 22: Static three-point bend test [5]

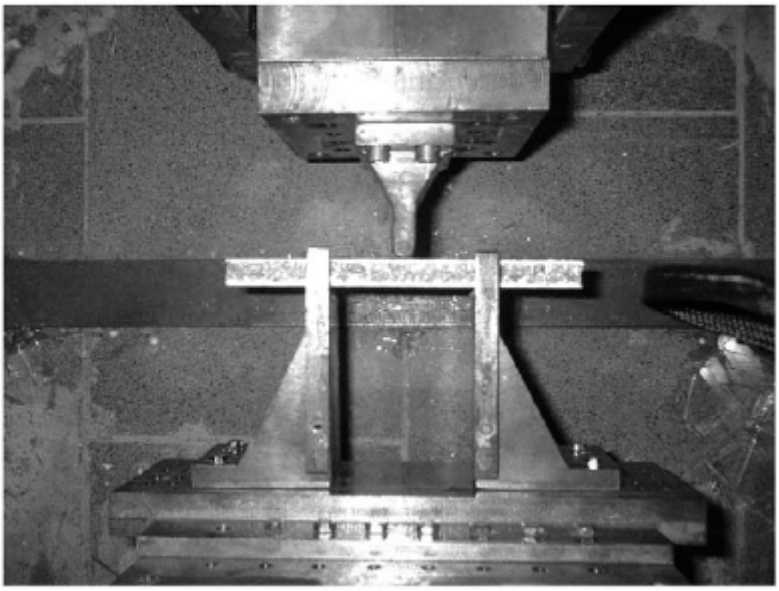

Figure 23: Dynamic three-point bend test [5]

The following quantities were measured during each test: force, acceleration, horizontal displacement and impact velocity. Data were simultaneously sampled by a 24 bit DAQ card with 40 KHz sampling rate. Digital images and videos were recorded and were used for investigation of different collapse mechanisms. From the following load–displacement diagram for the AFS Schunk sample as illustrated in Figure 24, they identified that the initial linear elastic behavior point 1 is followed by an elasto-plastic phase until a maximum value is reached. This is represented by point 2 in figure 24. After the point 2, the load decreases and during this phase, the energy is dissipated by indentation which forms points 3 and 4 in the graph. The observed collapse mode differed from the conventional collapse mechanism as illustrated in Figure 25.

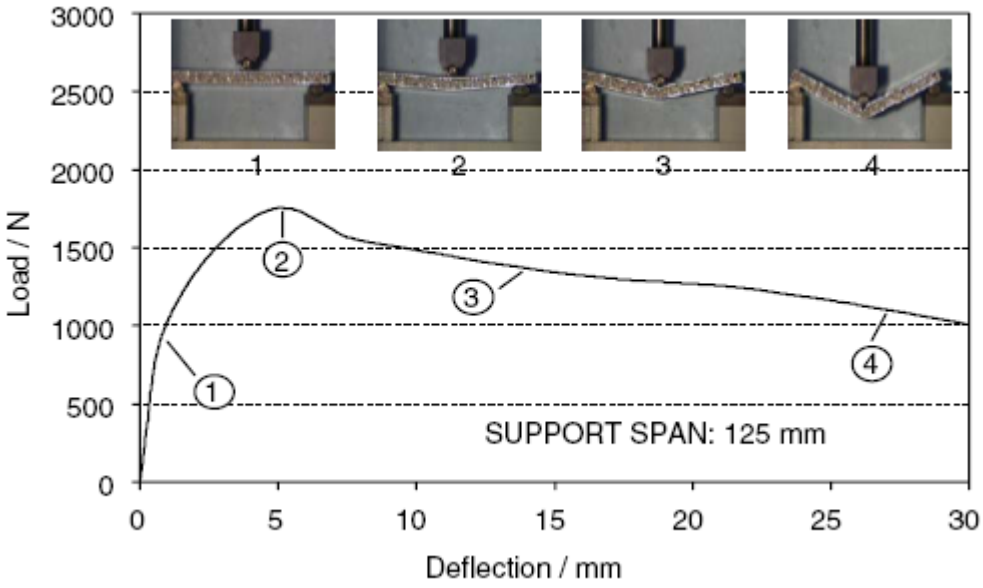

Figure 24: Load- deflection curve measured under static three-point bending [5]

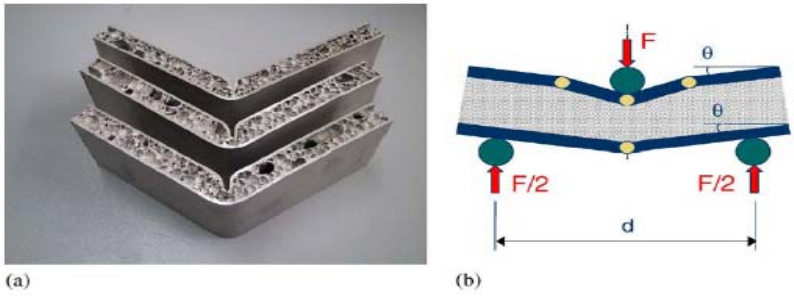

Figure 25: Collapse mode 1 (a) Experimental and (b) Theoretical model [5]

They decreased the span to 80mm to see the changes and the collapse mechanism changes as shown in Figure 26.

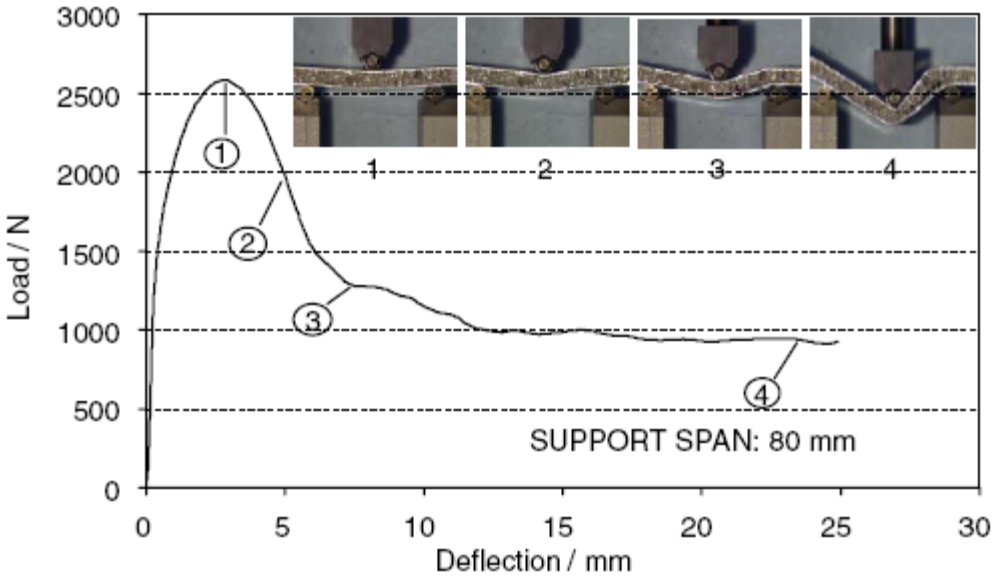

Figure 26: Load-deflection curve obtained by changing the span length in three-point bending under a static load [5]

They found that the behavior exhibited at point 2 in Figure 26 is due to core shear failure afterwards at points 3 and 4, the load almost remains constant and energy dissipation occurs due to the formation of plastic hinges shown in Figure 27 below.

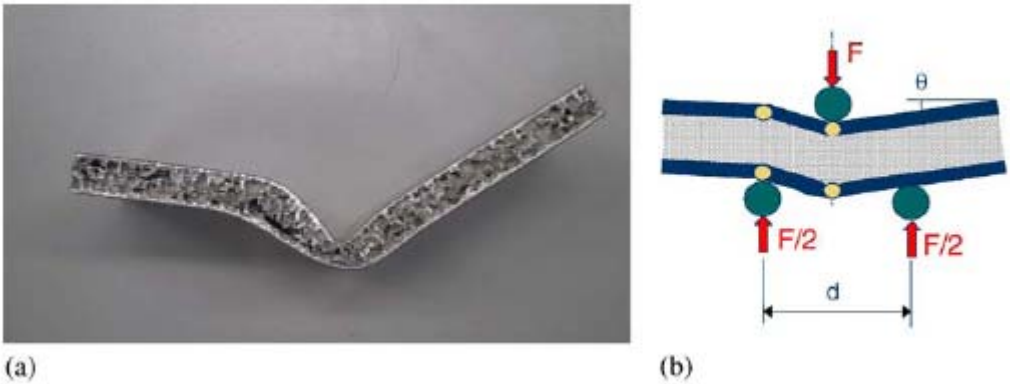

Figure 27: Collapse mode 2 (a) Experimental and (b) Theoretical model [5]

Thus, they proposed that in three-point bending, the Schunk sandwiches with span lengths greater that 90 mm are always collapsed by Mode 1 and sandwiches with span lengths less than 80 mm are collapsed by Mode 2A. At a span length of 90 mm, they witnessed Mode 1 collapse two times and Mode 2A collapse one time. For the alulight foam sandwiches, only one collapse mode 2b was observed in static three-point bending tests. When they changed the support span to a range of 55 to 135 mm, failure was due to the core shear. The effect was observed in the load-displacement diagrams. Theoretical modeling was done on these sandwiches.

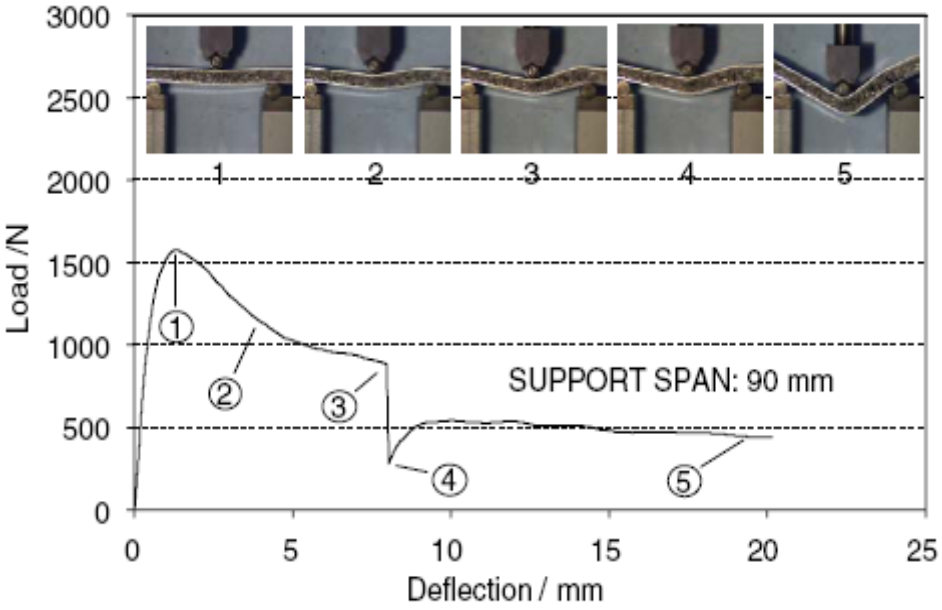

Figure 28: Load- deflection for alulight sandwich under static three-point bending [5]

In this way V.Crupi et al. pointed out the different collapse mechanisms for Shunk and Alulight sandwiches in three-point bending when the span length was changed. Mode 1, Mode 2A collapse mechanisms were obtained depending on the support span used and the properties of the AFS panels.

2.8 Response of syntactic core to three-point bending

In July 2002, Nikhil Gupta et.al. studied the response of the syntactic foam core sandwich structured composites in three-point bending [6]. The use of syntactic foam cores in sandwich composites is a relatively new application. These kinds of cores provide a smoother surface than the other available types of cores. They have a closed cell structure and are fabricated by mechanical mixing of hollow particles with matrix resin. The structure of syntactic foams is shown in Figure 29.

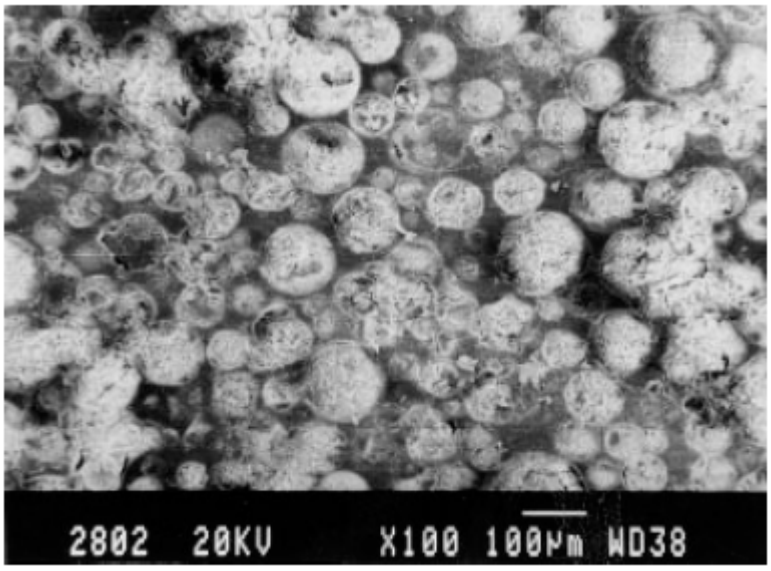

Figure 29: Scanning electron micrograph of syntactic foam cores [6]

The syntactic foam core material was fabricated by mixing hollow glass spheres with epoxy resin system followed by un-pressurized casting. The average particle diameter, average wall thickness and true particle density of the hollow glass spheres were $80\,\mu m$, $1.5\,\mu m$ and $254\,kg/m^3$ respectively. The syntactic foam cores were slabs with the following dimensions length-150mm, width-150mm and thickness-25.4mm. To fabricate the sandwich composite, four slabs of syntactic foams having an average density of about $445\,kg/m^3$ were chosen.

The compressive strength of the syntactic foam was found to be 20.5MPa. A stress-strain curve was drawn for the compression testing which is shown in Figure 30 below.

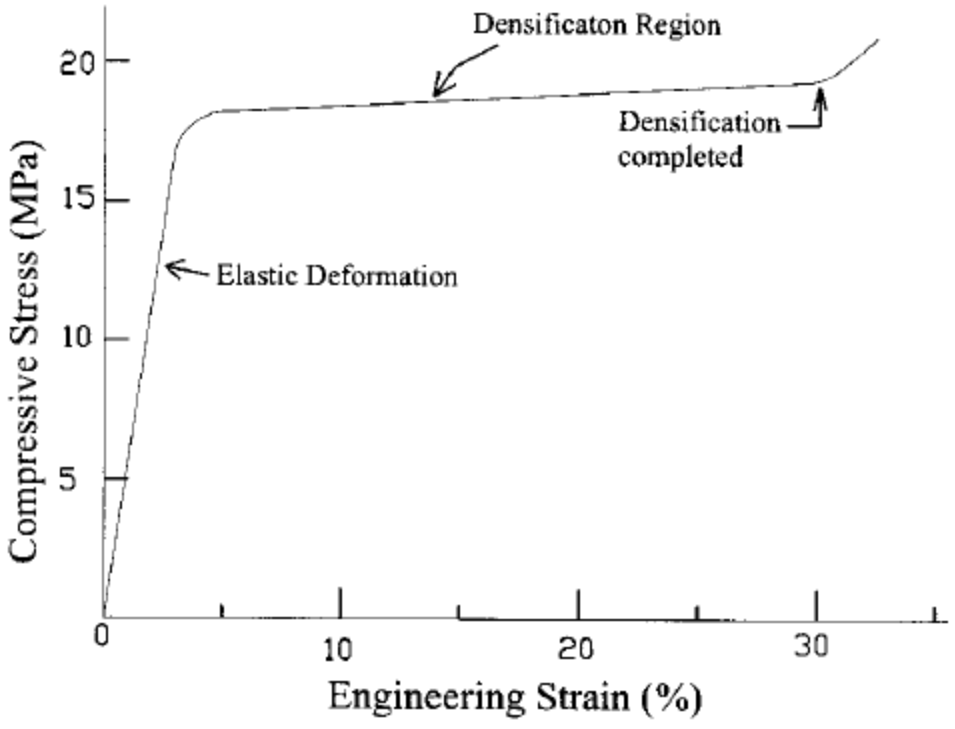

Figure 30: Stress- Strain curve for the compression of the syntactic foam core [6]

The “densification region” as marked in Figure 30 looks like a plateau region, which is a typical characteristic feature of the syntactic foam cores, and it corresponds to the energy absorption by the material in compression.

A thickness of 0.2 mm E-glass fabric was used as the reinforcement in two of the four fabric slabs. The glass fabric had an epoxy coating with a satin finish. The skins were bonded to the core material by a process called lamination. They, then, did some hand lay up followed by vacuum bagging to ensure good bonding between the skin and the core. The resin system used to manufacture the syntactic foam slabs was used in the fabrication of skins also. Non-destructive tests like Ultrasonic imaging (c-scan) was done to assess the quality of the fabricated sandwich panels and to check for cracks and damages in the core materials. Ultran NDC 7000 water immersion equipment was used for non destructive evaluation as illustrated in Figure 31.

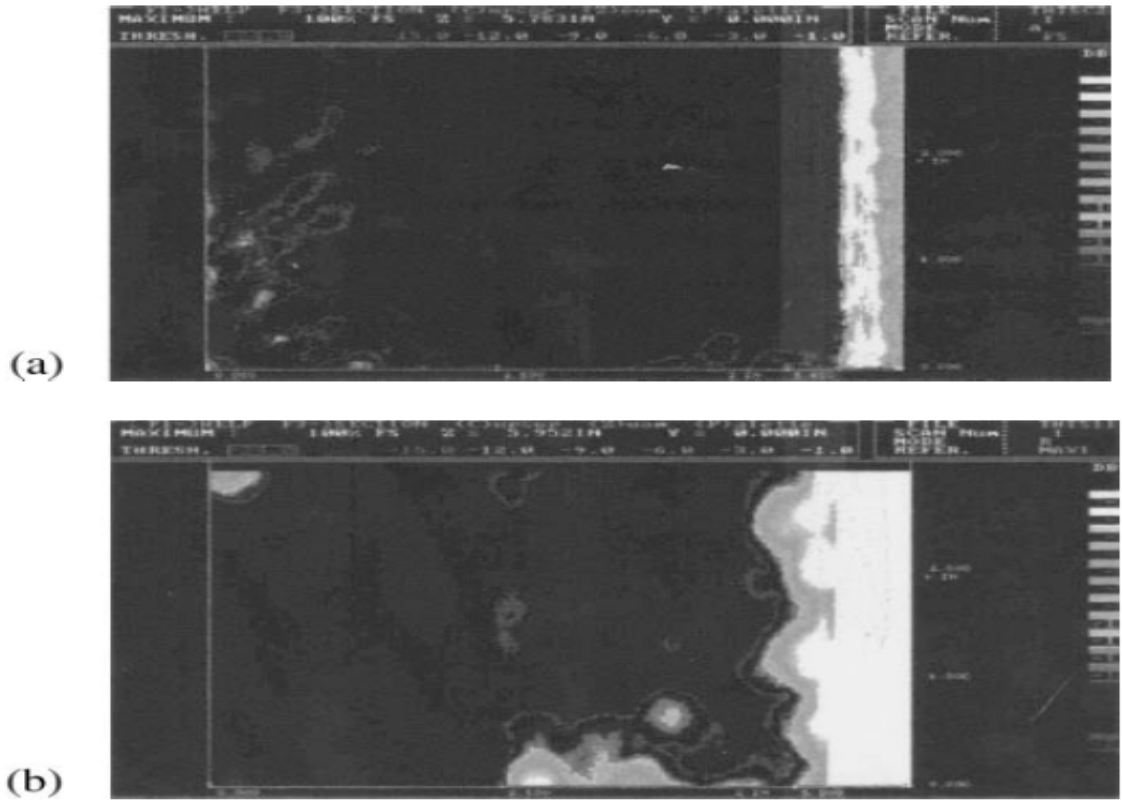

Figure 31: Results of Ultrasonic testing of two sandwich panels [6]

Theoretical analysis was done to derive the formulae for syntactic foam cores. A series of three- point bend tests were conducted with a 100 KN on INSTRON-8032 using a servo-

hydraulic microprocessor was used. The flexural and short beam shear tests were conducted on specimens with two different aspect ratios (length to thickness) of 16:1 and 5:1, respectively. The length and width of the specimens were 130 and 13mm, respectively. The tests were done at a constant cross head rate of 0.02 mm/sec and the span length used was 100 mm. Load–displacement plots were obtained for these tests for flexural analysis. The symbols and notations used for this experiment are illustrated in Figure 32.

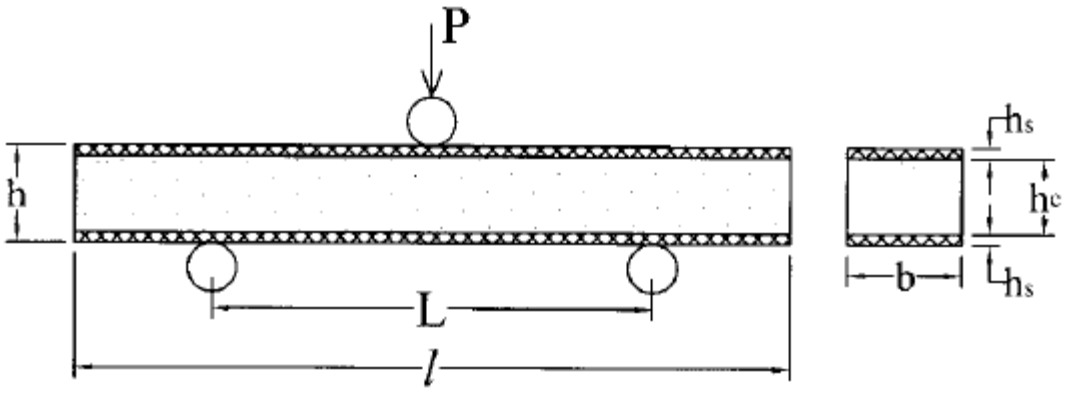

Figure 32: Symbols and notation used [6]

The specimen dimensions corresponding to t:L:l were 1:5:7 where t, L, l are specimen thickness, span length and total length respectively. The span lengths used in this case were 33mm for glass fabric skin and 31mm for glass- carbon hybrid skin. The width of the specimens used was 10 mm. The relation used for calculating bending stress in three-point bending was:

$$\sigma = \frac{PL}{2h_s\left(h+h_c\right)b} \quad - \quad (2.18)$$

The relation used for calculating shear stress under three-point bending was:

$$\tau = \frac{PL}{\left(h+h_c\right)b} \quad (2.19)$$

These tests indicated that structural performance was dependent upon the aspect ratio and the span thickness. Four random curves were chosen by Nikhil Gupta et al. for this plot and was found that three of the curves were almost similar in nature. Figure 33 illustrates the curves obtained from three-point bending of a syntactic foam core sandwich composite.

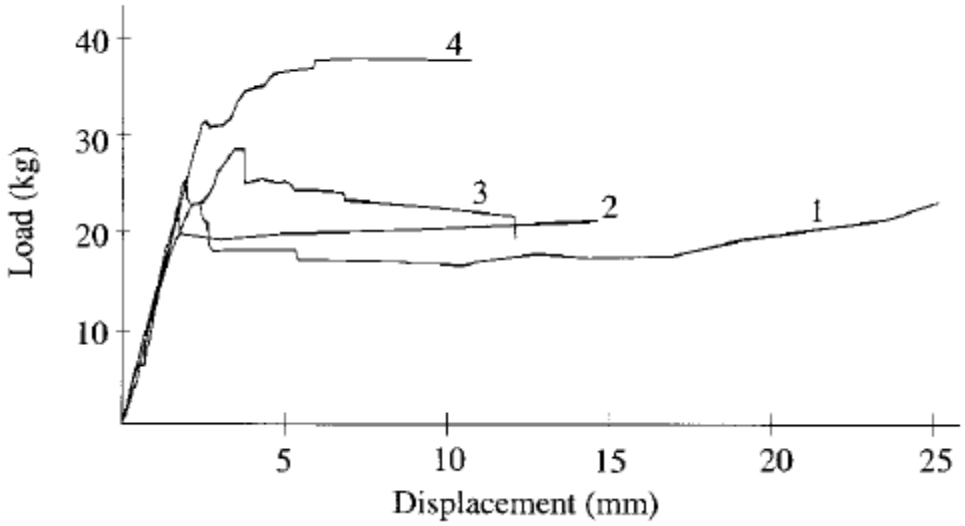

Figure 33: Curves obtained from three-point bending of syntactic foam core sandwich composite [6]

A generalized curve was drawn using the other curves obtained from the three-point bending test of syntactic foam core sandwich composite. The curve is good for both skins, i.e., glass and glass-carbon hybrid fabric. Figure 34 is divided into four regions. The first region, which is linear by appearance, shows the elastic deformation of the sandwich material. Region two corresponds to the plastic region, which is obtained right after the elastic region. The load in this region reaches the peak value followed by a sudden drop of 15 to 25% of the load in the next region. This sudden drop in load corresponds to load transfer due to the onset of fully plastic deformation and general failure of the face sheets. The resulting high core compressive stresses (region 3) results in crushing of the core micro balloons as illustrated shown in Figure 35.

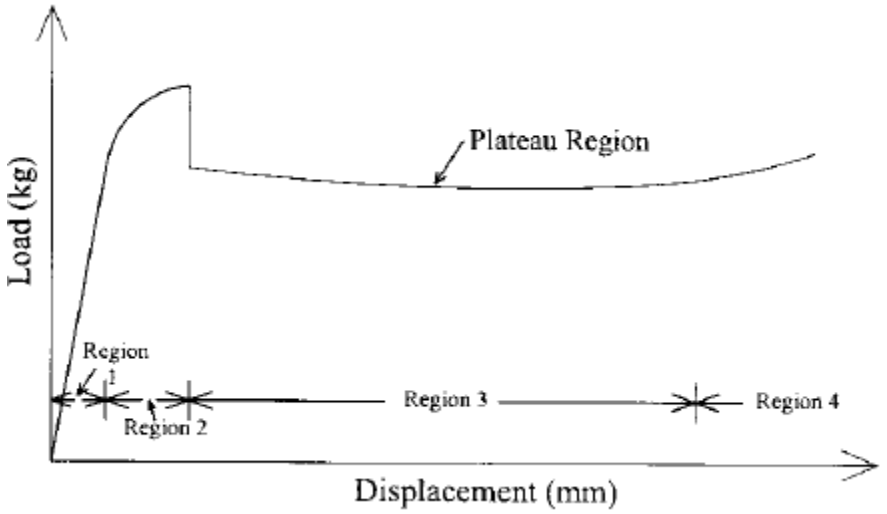

Figure 34: Proposed load-displacement curve based on curves obtained during the flexural testing of syntactic foam core sandwich composite [6]

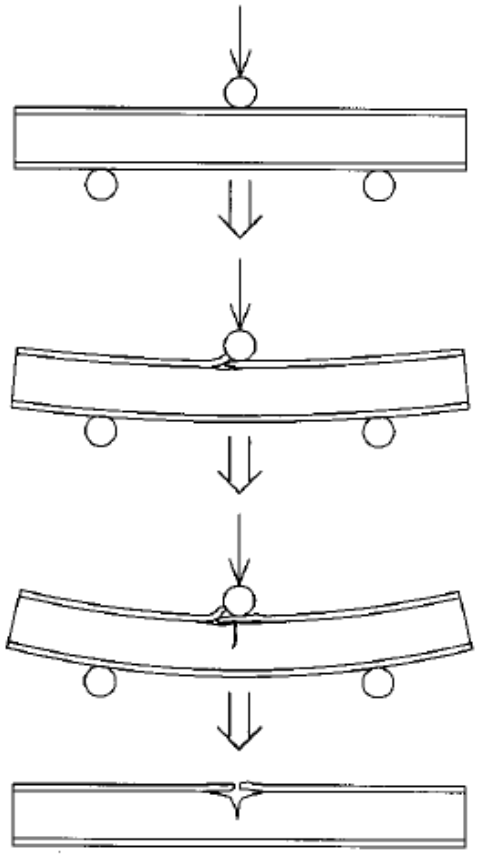

Figure 35: Failure sequence of syntactic foam core composite sandwich in flexural testing [6]

The plateau region is also an indication of a dynamic equilibrium of the volume created due to the crushing of micro balloons in the core. When this process completes, the load slowly starts increasing, this is shown as region 4 in Figure 34.

Short-beam shear tests can estimate the shear strength of sandwich structures. Load–displacement curves were recorded for the short beam test also as illustrated in Figure 36. The load-displacement curves obtained from this test (figure 36) show a variety of curves having different shapes. To make a more generalized study, these curves were generalized into a single curve.

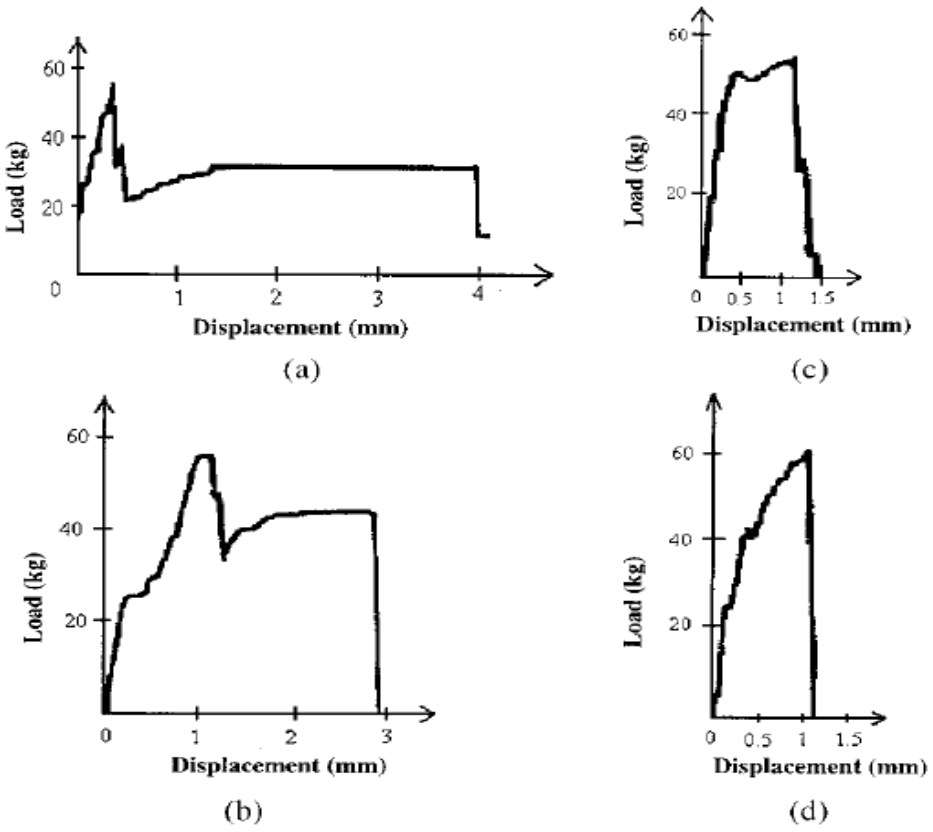

Figure 36: Load –deflection curves obtained from short beam shear tests [6]

A generalized curve derived from the actual load-displacement curves is shown in Figure 37. Nikhil Gupta et al. analyzed it in three separate regions. The first and second regions correspond to elastic and plastic regions, respectively. At the end of the second region, the load drops suddenly from the maximum value due to the fracture on the tensile side of the sandwich structure. The drop in the load was found to be 30 to 50% of the maximum recorded load. They noticed that the failure came as a result of a small part of core sticking to the skin and getting separated rather than the critical interface failure. In some cases, the core failed well away from the critical interface.

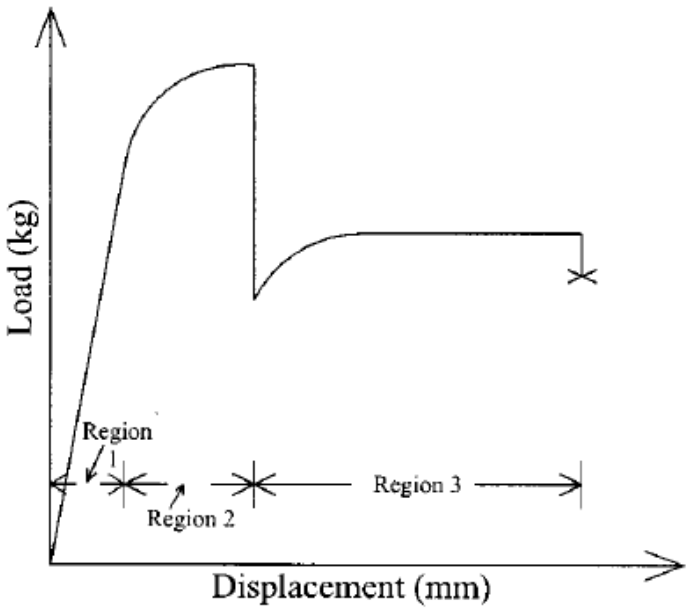

Figure 37: A generalized curve analyzed and drawn from all the above four curves [6]

The observation was interpreted in the form of the interfacial shear strength between skins and core is higher than shear strength of the syntactic foam used as core material.

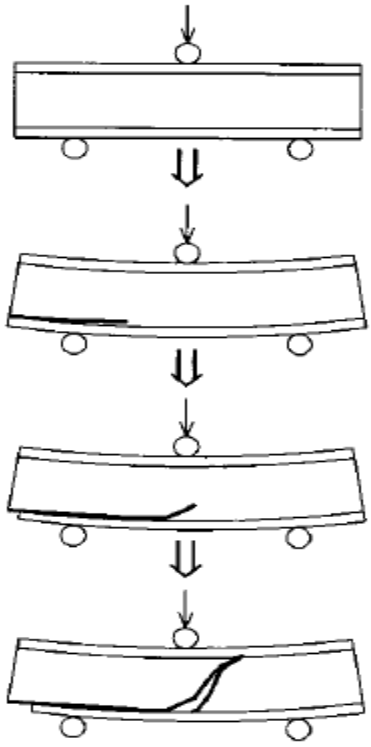

Figure 38: Failure sequence of sandwich composites in short beam shear test [6]

At the point of interfacial failure, the load is transferred to the core and if the load is higher than the strength of the core, it also fails at the same instant. Failure mode of the sandwich structure materials tested under flexural conditions can be summarized as skin micro buckling followed by compressive failure of the core material.

They finally concluded by saying that the aspect ratio of the test specimens plays a critical role in determining the failure of the specimen. In the flexural tests, the failure was a skin failure due to micro buckling followed by the compressive failure of the core. Failure obtained from the shear tests was shear cracking of the core followed by failure in tensile mode. Scanning electron microscope observations also support these observations. These observations were found to be consistent for both types of skins, glass and glass carbon hybrid fabric.

This is a promising experimental and analytical model for the analysis and study about the syntactic foam core sandwich structure and is also suitably modified to make it apply for most of the foam type of hollow-filled materials.

Chapter: 3 Experimental and Analytical Procedures

3.1 Three-Point Bending

Sandwich composites can be made in to beams and solid mechanics can be applied to the analysis. Analysis can also be done on sandwich composite response to loading in various failure modes. Classical beam theory states that the strength of a solid structure is a function of the cross sectional area of the structure. One of the most common types of test used for testing of composite panels for their mechanical properties is a three-point bending test. It can be performed on regular rectangular composite panels with simple apparatus. In tensile testing, there is a transfer of load at the specimen grip which can be avoided in a three-point bend test. The tensile test will give accurate properties for Young's Modulus and tensile strength of a material. This type of test will also give you inter laminar shear strength of curved specimens. The shear strength can be calculated by using the same equations used for bending of prismatic bars. These properties govern the eventual strength of the specimen and are the function of the amount of compressive force used while the specimen was first made. However, this test also has some disadvantages.

The primary disadvantage is that the stresses in specimens subjected to three-point bending are inherently non uniform and vary in kind i.e. tension on one side of the specimen and compression on the other side making the results comparatively harder to interpret than any of the uni-axial tests. The test is also open to the violations of specimen geometry and the details of the loading system which can affect the results. One advantage of the disadvantages of the test depends on its use. If the testing is done for specification or quality control purposes, it is

relatively unimportant because then the test is just a comparative study and it has to meet the requirements for the comparability of results which can be satisfied by prescribing any one set of test conditions chosen arbitrarily from a big range of values. A schematic of a thee-point bending test is illustrated in Figure 39

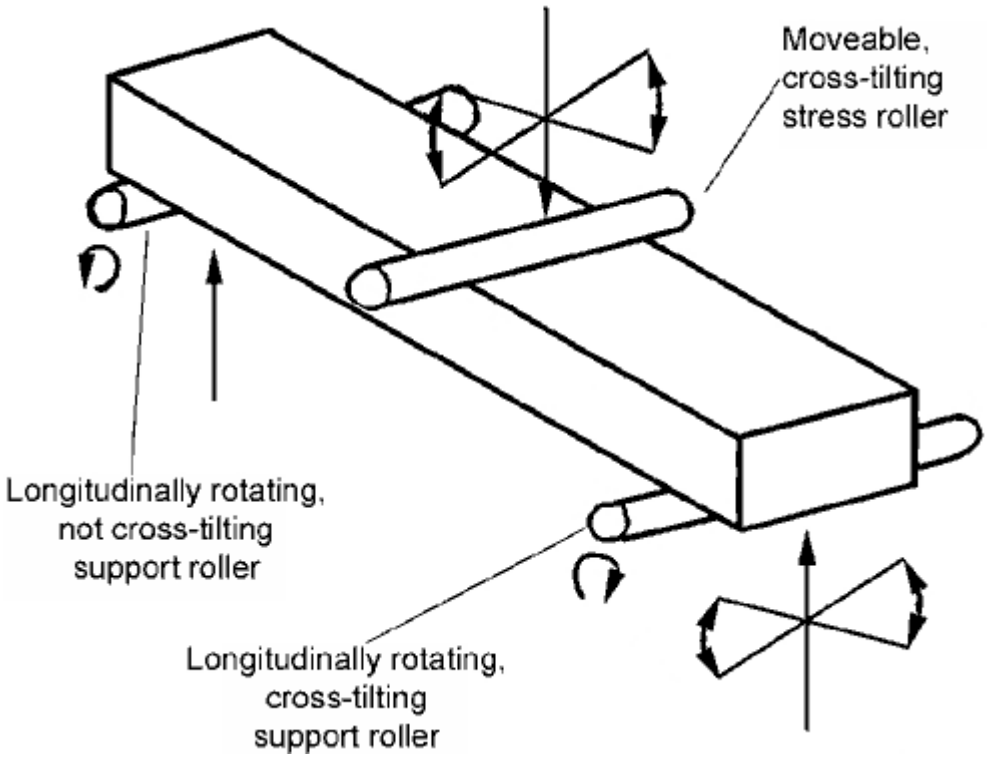

Figure 39: Three-point bending [14]

If the basic mechanical properties need to be found out instead of comparing the results, more care should be taken while doing the experiment and the experiment performed will be more difficult.

There is also a systematic need for analysis of the variables involved in the three-point bending test. In this type, damage initiation and propagation of loads are very close to each other and failure has a more catastrophic nature than in the four point bend test. This is because once a

crack is formed, the bending moment in the skin at the crack front increases and the crack propagates while in four-point bending, it remains constant. The four-point test and the five point bend tests are less popular inspite of their technical advantages over the three-point bend test.

The three-point bend test is usually done on MTS (Material Testing System) machine or an Instron machine. Every test performed on MTS machine or an Instron machine needs test fixtures to hold and support the specimens. In three-point bending, the three-point bending test fixtures are used.

3.2 Material Testing System Machine

The three-point, four-point and five-point bending tests can be done on an MTS machine. MTS is Material Testing system and there are one or more companies manufacturing MTS machines. Two of the companies manufacturing MTS machines are "Material Testing System" and "Instron." These two companies in turn have many models of their own MTS systems. The MTS machine setup can be found in Appendix 1: MTS Machine Setup. Figure 40 below shows Micro Console, Controllers and Micro profiler

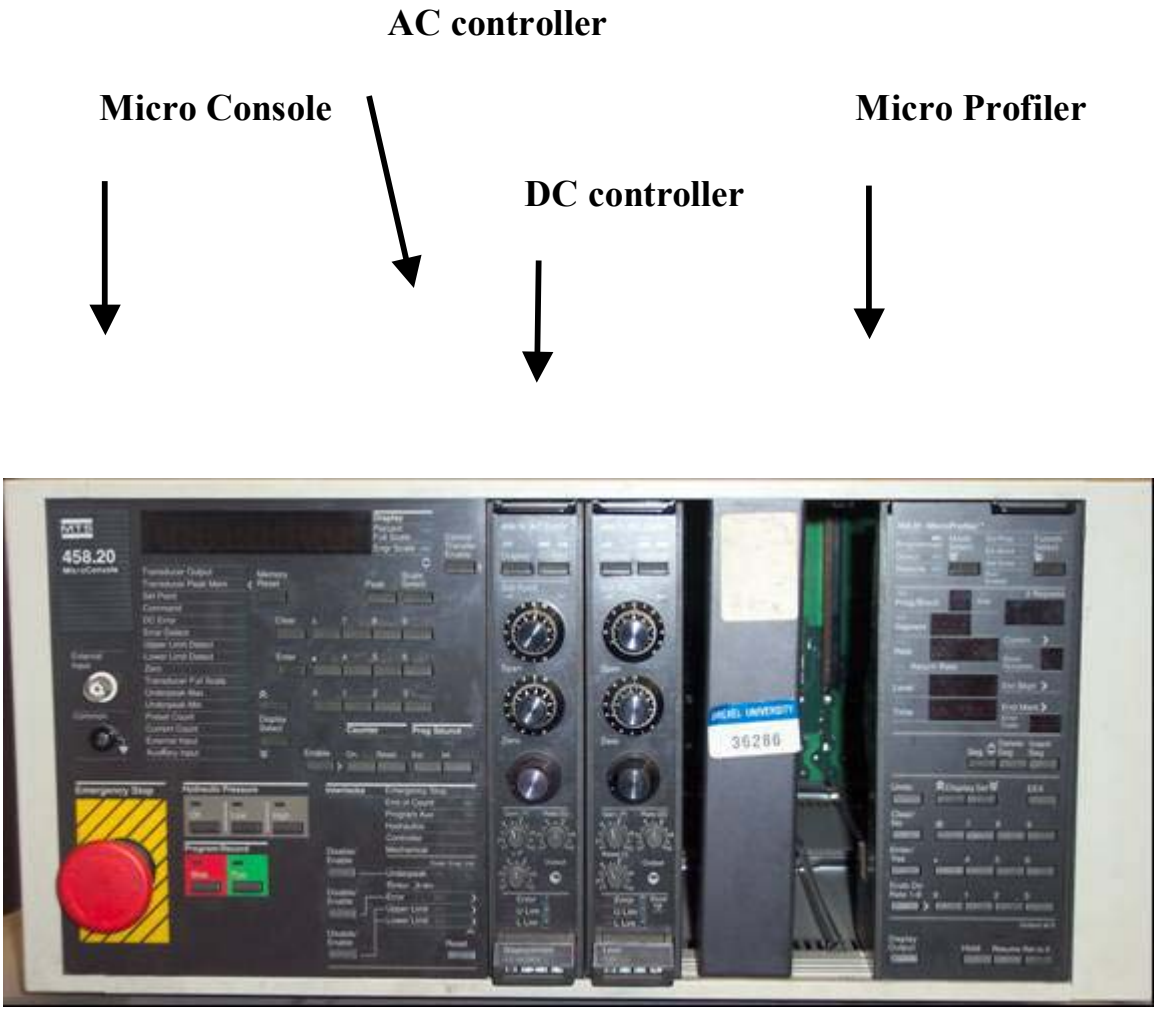

Figure 40: Micro Console, Controllers and Micro profiler

There is a control panel for the MTS machine to record the test data. The three-point bending was done on Instron 8562 testing machine shown in the Figure 41. This machine had an Instron 8500 Electronics control panel which is the control system for operating the MTS machine. The machine was equipped with Hewlett Packard 34970 A Data Acquisition System switch unit. The data acquisition system is for recording the test data from the machine as illustrated in Figure 42. Different data acquisition systems use different softwares to record and

store the data. The wheat stone bridge was also connected to the machine to increase the gage sensitivity.

Figure 41: MTS Machine (INSTRON type) and its control panel

	Model	SN	
Frame	A1477-1004	H0708	
Actuator	A726-45B, IDC 272	210	±124 KN static ± 100 KN dynamic
Stroke			±50 mm
Servovalve	110-3-1074 (Moog 760-723A)	231	
Load Cell	2518-611	UK517	±200 KN static ± 100 KN dynamic
Grips	2742-404		water cooled side entry wedge grips
Column Clearance			660 mm
Maximum Clearance with grips			800 mm
Electronics	8500	V11.0/V11.1/V11.0/V11.0/V11.0	
Electrical Power Pack	A1663-1007		

Table 3.1: Details of INSTRON 8562

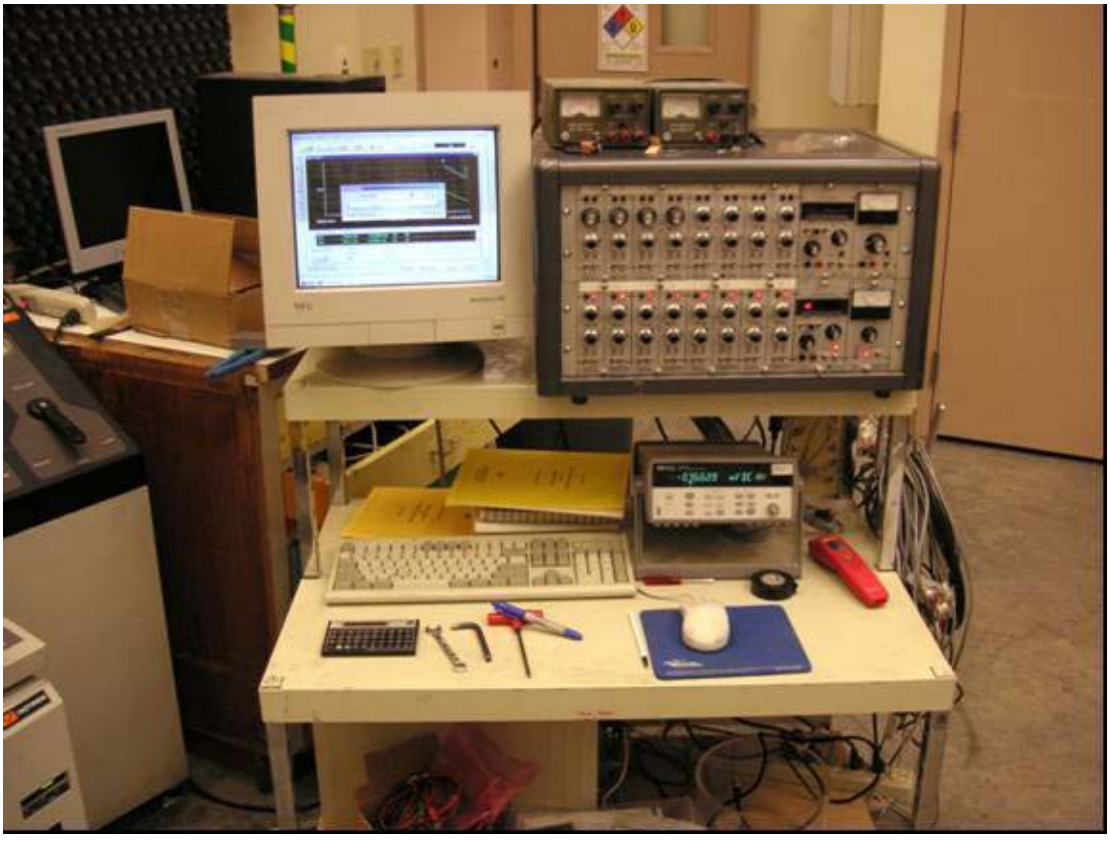

Figure 42: Wheatstone bridge connected to the MTS Machine

3.3 Finite Element Analysis

Finite Element Analysis (FEA) is a computer simulation used in engineering analysis. It was first developed by Richard Courant in 1943 who obtained approximate solutions to vibration systems by using RITZ method of numerical analysis. It has been continuously improved and developed since then. Development of Finite Element Model in structural mechanics is usually based on an energy principle such as the virtual work principle or the minimum total potential energy principle. In the finite element analysis, the object is represented by geometrically similar model constituting of single or multiple, linked objects and representations of discrete regions called finite elements (dividing the actual structure of the geometry in to collection of discrete elements). The elements are joined by shared nodes and the collection of nodes and finite elements is called a mesh. The boundary conditions i.e. compatibility and constitutive relations are applied to each element and a system of simultaneous equations is constructed. The efficiency of the model depends on the mesh created before solving the model. By refining the mesh of the model, improved and effective results are possible. The most common use of FEA is the determination of stresses and displacements in mechanical objects. It is also used in heat transfer and fluid dynamics. It can solve very complex cases like closed form analytical solutions.

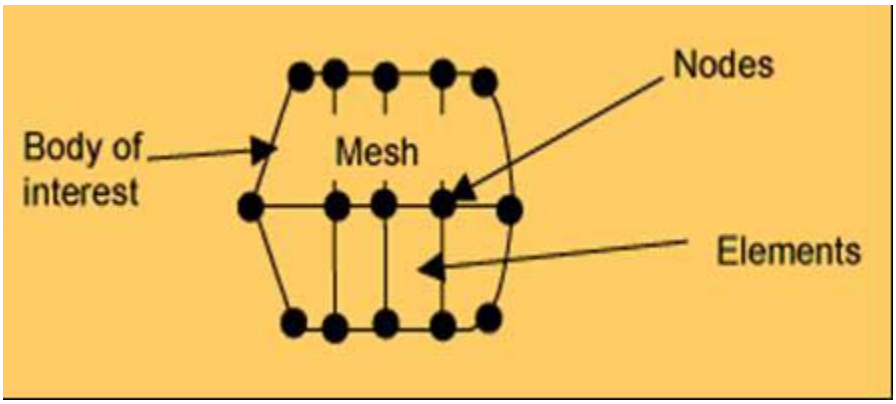

Figure 43: The Schematic of nodes, elements and mesh [14]

In the stress analysis problem, finite element software calculates the displacement of the nodes and from this information, stresses and strains on the mechanical object can be calculated.

3.4 I-DEAS Software

I-DEAS ("Integrated Data Evaluation and Analysis System") was utilized for verifying results obtained from the testing program. This software combines a wide variety of engineering tools for design and Finite Element Analysis. The ability to develop products with CAD/CAM/CAE technology has made it possible to understand fully about the products from a manufacturing point of view.

Chapter 4: Analytical Formulae

4.1 Stiffness, shear modulus and deflection of sandwich beams in three-point bending

Consider a simply supported sandwich beam in three-point bending as shown in Figure 44. The mid point of the beam deflects by a transverse displacement of 'w" when a vertical load of 'P' acts on midpoint of the sandwich composite beam. Let the span length between the two supports be 'a', 'b' the width of the sandwich coupon, 'c' the core thickness, 'h' the total thickness, 'P' the total load applied at the midpoint of the sandwich beam, 'f' be the thickness of the facing, 'E_f' be the Young's modulus of the facings, 'E_c' be the Young's modulus of the core, 'G' be the core shear modulus, 'D' be the flexural stiffness, 'N' be the shear stiffness, 'S' be the core shear stress and 'F' be the average facing stress.

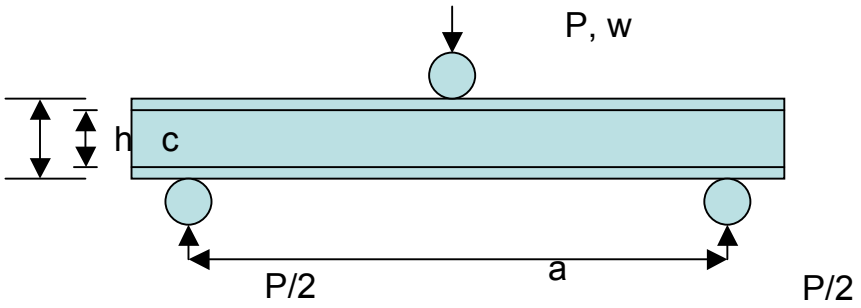

Figure 44: Three-point bending of a simply supported sandwich beam

Flexural Stiffness:

$$D = E_f (h^3 - c^3) b / 12L \tag{4.1}$$

Where

$L = 1 - \upsilon^2$, υ is the Poisson's Ratio of the facings, υ=0.33

Shear Stiffness:

$$N = G(h + c)^2 b / 4c \tag{4.2}$$

A lot of studies have been conducted on the collapse mechanisms of sandwich beams in three-point bending. The following are some modes of collapse which are usually identified in three-point and four point bending. Figure 45 shows the collapse modes in sandwich beams.

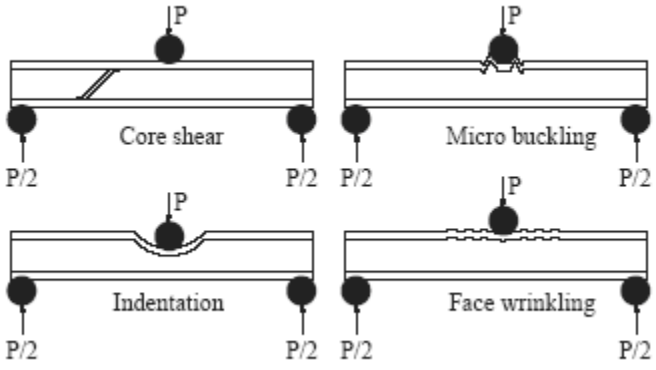

Figure 45: Failure modes of sandwich beams in three-point bending [15]

Core Shear Stress:

$$S = \left[P / \left(h + c \right) b \right]^{k} \tag{4.3}$$

Where

K= constant (assumed 1 from ASTM C 393).

Average Facing Stress at Mid span Load:

$$F = P * a / 2 f (h + c) b \tag{4.4}$$

Mid span Deflection:

$$W = (Pa^3 / 48D) + (Pa / 4N) \tag{4.5}$$

Chapter 5: Experiments and Results

5.1 Experiment 1

The experimental component of this study discusses the dimensions of the sandwich composites, and the three-point bending tests on a balsa wood core composite sandwich.

The materials and their dimensions were obtained from the US Army for the first phase of testing.

Table 2: Balsa wood core- glass fiber polyester composite panels as received for testing

Code	Material	Length, in	Width, in	Thickness, in
PKD-AL 1	Aluminum Honey comb	12	6	7/16
PKD-AL 2	Aluminum Honey comb	12	6	7/16
PKD-AL 3	aluminum honey comb	12	6	7/16
PKD-BL1-(3/4)	balsa wood core sandwich	12	6	¾
PKD-BL2-(3/4)	balsa wood core sandwich	12	6	¾
PKD-BL3-(3/4)	balsa wood core sandwich	12	6	¾
PKD-BL4-(3/4)	Balsa Wood Core sandwich	12	6	¾
PKD-BL5-(3/4)	balsa wood core sandwich	12	6	¾
PKD-BL6-(3/4)	balsa wood core sandwich	12	6	¾
PKD-BL1-(1)	balsa wood core sandwich	12	6	1
PKD-BL2-(1)	balsa wood core sandwich	12	6	1
PKD-BL3-(1)	balsa wood core sandwich	12	6	1
PKD-BL4-(1)	balsa wood core sandwich	12	6	1
PKD-BL5-(1)	balsa wood core sandwich	12	6	1
PKD-BL6-(1)	balsa wood core sandwich	12	6	1

These panels were fabricated into small rectangular specimens according to ASTM C 393 standard for flexural testing of sandwich composites as illustrated in Figure 46.

A schematic for balsa wood core composite sandwich, thickness= 0.745 in.

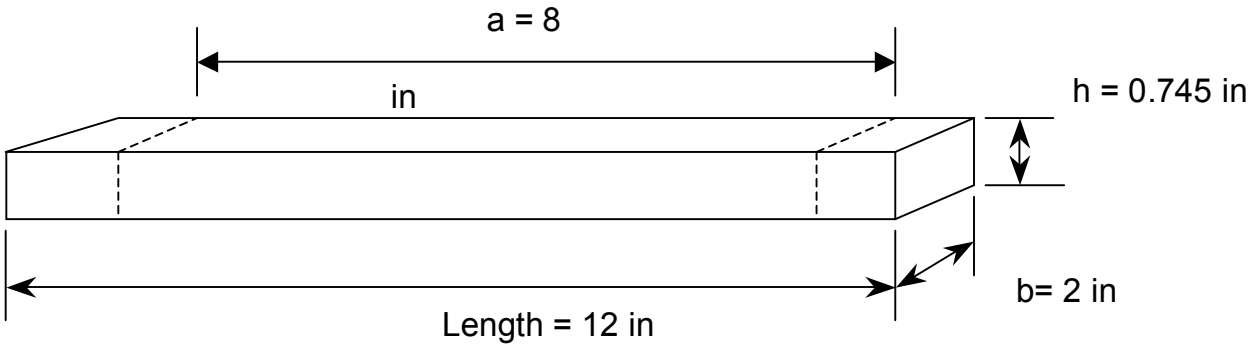

A schematic for balsa wood core composite sandwich, thickness= 1 in.

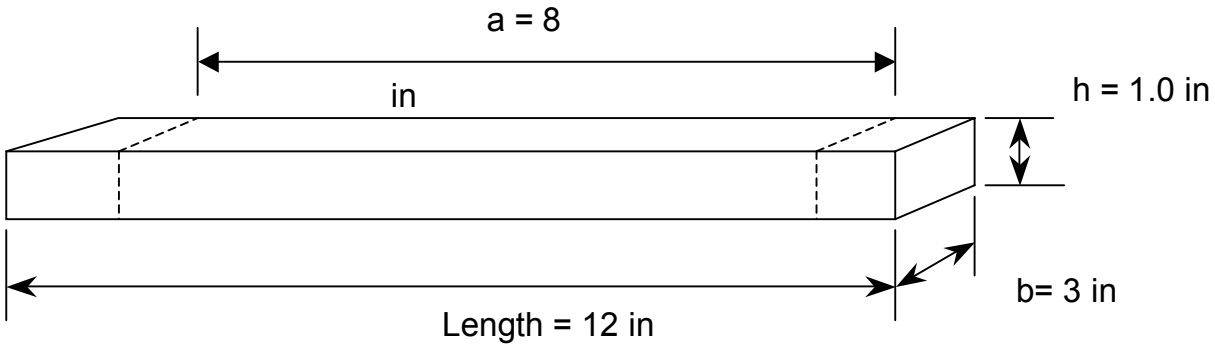

Figure 46: Dimensions of balsa wood- glass fiber polyester specimen tested

5.11 Testing of balsa wood core composite sandwich with glass fiber polyester facings

Balsa wood with a modulus of elasticity 17259 psi was used for the experiments. Balsa wood core composite sandwich coupons with glass fiber polyester facing plates were used as test coupons. Three-point bend tests were performed at room temperature on Instron 8562 test machine. 10, 1 inch thick balsa wood core composite sandwich coupons and 14, ¾ inch thick balsa wood core composite sandwich coupons were tested at room temperature using a three-point bend test. Figure 47 shows the three-point bend test at room temperature. The dimensions of the specimens were 12inch x 3inch x 1inch and 12inch x 2inch x ¾ inches. The load-deflection data was recorded from the Instron 8500 Electronics control panel. The displacement rate provided to the piston was 0.005 in/ sec. Strain data was recorded for only four specimens of which two of them were 1 inch thick. Tensile strains were measured using strain gages mounted on the bottom side of the specimen.

Figure 47: Three-point bending of balsa wood core composite sandwich

5.12 Observations

The typical measured responses are reported here. The face plates were much stronger than the core (balsa wood). The failure obtained from the experiment was a catastrophic failure of the core, which is due to high core shear. The maximum load recorded on the MTS machine for 1 inch thick balsa wood core composite sandwich was 1131.23 pounds and the maximum deflection at the point of maximum load was 0.1833 inches and the maximum load for ¾ inch thick balsa wood core composite sandwich was 603.275 pounds and the maximum deflection recorded was 0.21042.

Analytical results are calculated from the formulae in chapter 4 and they are in close connection with the experimental results. Figure 48 illustrates a load-deflection plot for a 1 inch thick balsa wood core composite sandwich.

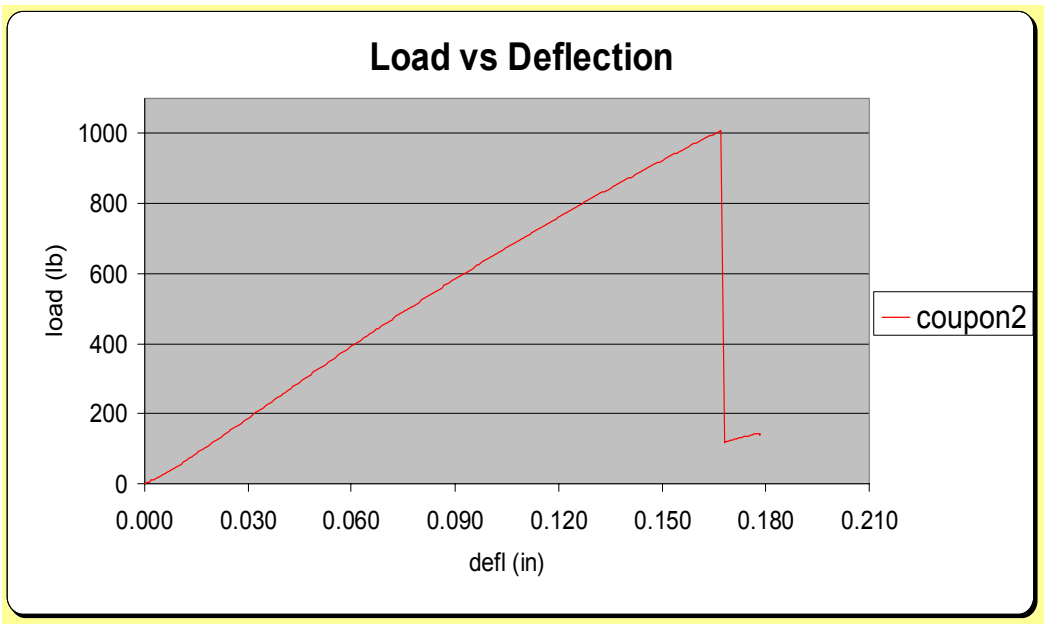

Figure 48: Load–deflection plot for 1 inch balsa wood core composite

5.2 Experiment 2

The following table shows balsa wood core-glass phenolic composite panels as received for the second phase of testing at room and elevated temperature.

Table 3: Balsa wood core-glass phenolic composite panels as received for testing

Type of Panel/ Geometry	Length as received (in)	Width as received (in)	Thickness as received (in)	Length as measured (in)	Width as measured (in)	Avg. thickness measured (in)
Dutta 1	12	12	0.57	12.00	12.00	0.55
Dutta 2	12	12	0.57	12.00	12.00	0.55
Dutta 3	12	12	0.57	12.00	12.00	0.55
Dutta 4	12	12	0.57	12.00	12.00	0.55
Dutta 5	12	12	0.57	12.00	12.00	0.55
Dutta 6	12	12	0.57	12.00	12.00	0.55
Dutta 7	12	12	0.57	12.00	12.00	0.55
Dutta 8	12	12	0.57	12.00	12.00	0.55
Dutta 9	12	12	0.57	12.00	12.00	0.55
Dutta 10	12	12	0.57	12.00	12.00	0.55
Dutta 11	12	12	0.57	12.00	12.00	0.55
Dutta 12	12	12	0.57	12.00	12.00	0.55

5.21 Testing of balsa wood core composite sandwich with glass phenolic facings

The Figure 49 illustrates the coupon obtained from a big rectangular sandwich panel after fabrication.

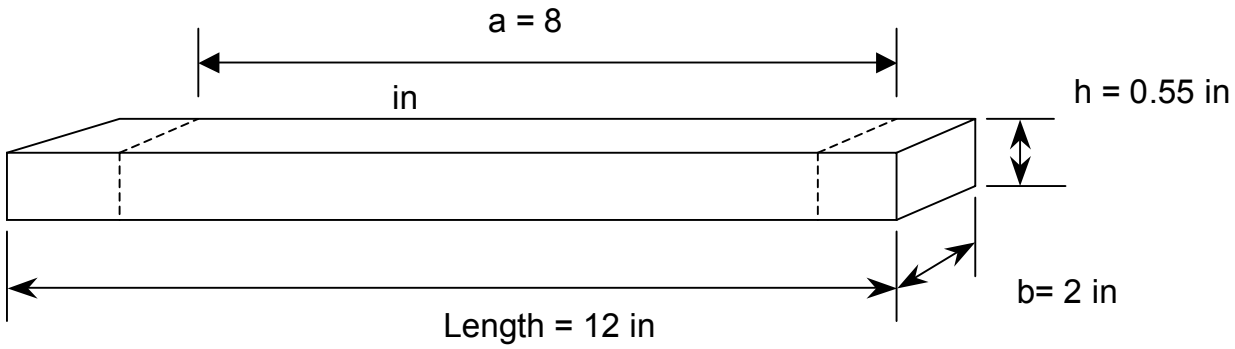

Figure 49: Dimensions of balsa wood- glass phenolic specimen

Three-point bending tests were done for balsa wood core composite sandwich with glass phenolic facings at room and elevated temperatures. Balsa wood of Young's modulus of 725000 psi was used for the experiments. Balsa wood core with glass phenolic as facing plates was used for test coupons. The testing was carried out on Instron 8562 test machine. 18, ¾ inch thick balsa wood core composite sandwich coupons were tested at room temperature and 36 of the same material coupons of same thicknesses were tested at elevated temperatures. The first phase of testing was done at room temperature. Figure 50 shows the three-point bend test at room temperature. The load, deflection data was recorded from the Instron 8500 Electronics control panel. A wheat-stone bridge was connected to the MTS machine to increase gage sensitivity. The displacement rate provided to the piston was 0.005 in/ sec. The span length used in both room and elevated temperature tests is 8 inches. Strain data was recorded for some of the specimens. Tensile strains were measured using strain gages mounted on the bottom side of the specimen. Precision strain gages were used which had a temperature range of -75 to +175 degrees Celsius and a resistance of 120.0(+ or -) 0.3% at 24 degrees Celsius. They were supplied with

encapsulated grid and exposed copper coated integral solder tabs which were suitable for stress analysis. Temperature was measured by a type-T thermocouple which is one of the most sensitive thermocouples available in the market. The elevated temperature tests were done at 61 degrees Celsius.

Figure 50: Three-point bending of balsa wood core composite sandwich with glass phenolic facings at room temperature

5.22 Observations

The typical measured and noticed responses are reported here.

1. At Room Temperature:

The face plates were much stronger than the core (balsa wood). The failure obtained from the experiment was a catastrophic failure of the core which is due to high core shear but

almost all the failures were noticed during the testing involved failure at the critical interface, skin failure, or core failure etc. The mean of the failure loads calculated after it was recorded on the MTS machine for balsa wood core composite sandwich at room temperature, was 300.4 pounds, and the maximum deflection at the point of maximum load was 0.250 inches. It was noticed that critical interface failure occurred whenever the coupon was failing at a lower load than normal. For loads above the normal failure load, skin failure due to tension or core failure due to high core shear was noticed. Figure 51 illustrates a load-deflection plot for balsa wood core composite sandwich with glass phenolic sandwich at room temperature.

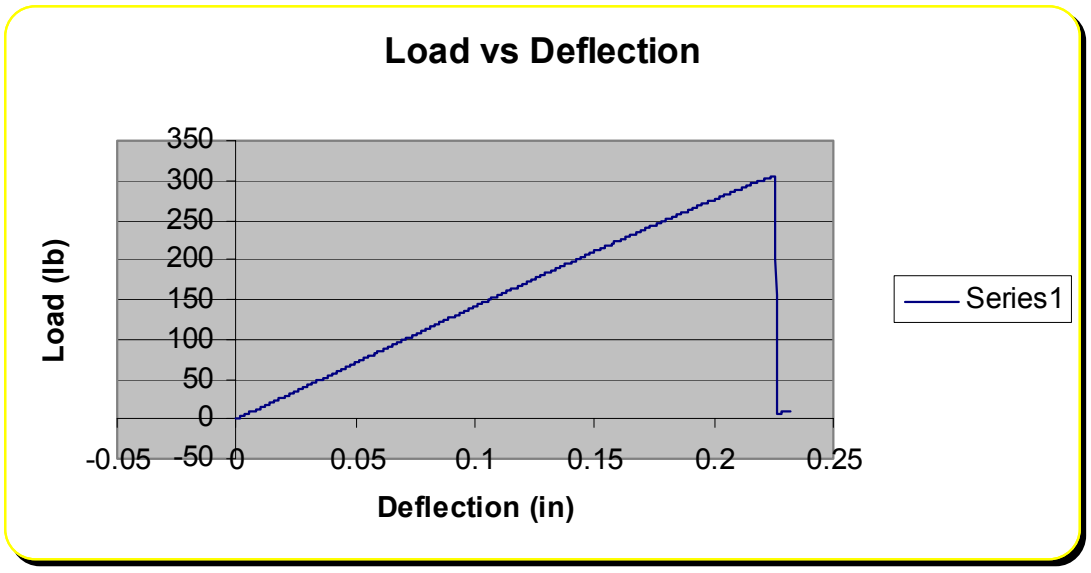

Figure 51: Load –deflection plot for balsa wood core sandwich with glass phenolic facings at room temperature

2. At Elevated Temperature:

Again, most of the time, the failure obtained from the experiment was a catastrophic failure. The mean of the failure load calculated after it was recorded on the MTS machine for

glass phenolic facing-balsa wood core composite sandwich, was 256.2 pounds and the maximum deflection at the point of maximum load was 0.281 inches.

For both room and high temperature testing, whenever the coupons failed at high loads, the failure came involved a small part of the core sticking to the skin and getting separated rather than the critical interface failure. In some cases, the core failed well away from the critical interface.

Things observed and proposed when core failed

1. The load got transferred to the core after the facing cracked.
2. At the point of interfacial failure, if the load is higher than the strength of the core, it also fails at the same instant. Failure mode of these kinds of sandwich structures can be summarized as skin micro buckling followed by compressive failure of the core material.

Figure 52 illustrates a load-deflection plot for balsa wood core composite sandwich with glass phenolic facings at elevated temperature.

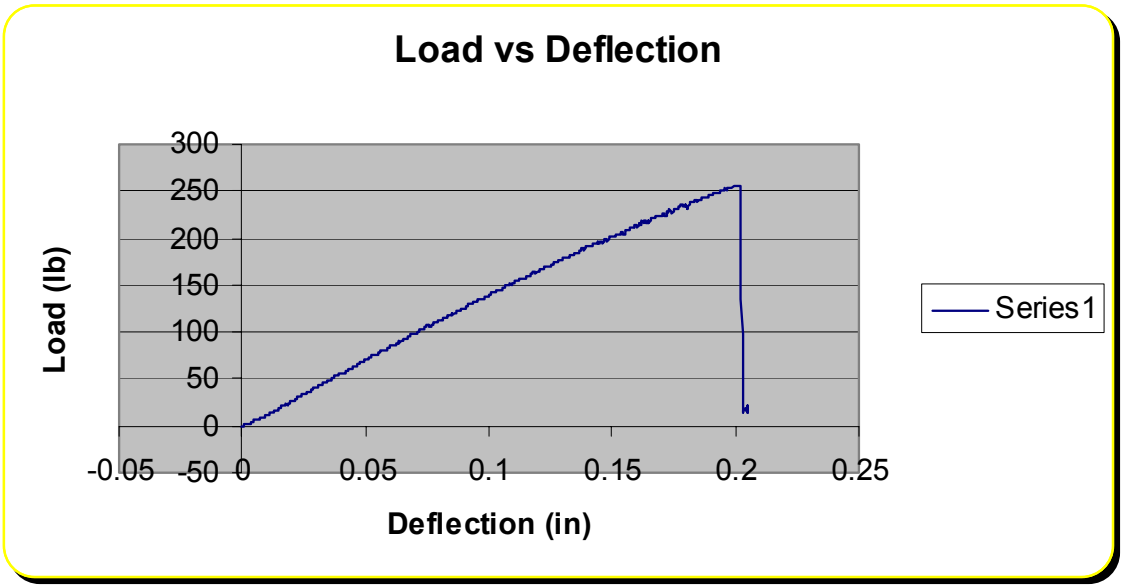

Figure 52: Load –deflection plot of "balsa wood core sandwich with glass phenolic" facings at elevated temperature obtained from a three-point bending test

Chapter 6: Analysis of the test data

6.1 Theoretical Analysis

Before the experiments were done, theoretical analysis was done to calculate the flexural stiffness, core shear modulus, average facing stiffness, shear stiffness, average facing stiffness and deflection of balsa wood core composite sandwich with glass polyester facings and the same sandwich with glass phenolic facings. The calculations were done using the formulae from the report [1]. Similar analytical calculations were done on balsa wood core composite sandwich with glass phenolic facings. The analysis was done to compare both analytical and experimental values, i.e., to check if the experimental values of deflection match with the theoretical values of deflection under the same failure loads.

6.2 Statistical Analysis

A statistical analysis was done using **MINITAB** software. A T-test was done on the test data for both room and elevated temperatures to ascertain if temperature was the factor in failure. The mean of the failure loads for the tests at elevated temperature was found to be 256.2 and the mean of the failure loads for the room temperature is 300.4. The standard deviation for both the tests at elevated and room temperatures were found to be 34.0 and 39.3, respectively. The S.E mean was found to be 5.7 and 9.3 for elevated and room temperature tests, respectively. The T-test also gives T-value, P-value and DF which were found to be -4.07, 0.0001, and 30, respectively.

6.3 Finite Element Analysis

A Finite element model was developed using I-DEAS software for balsa wood core composite sandwich with glass phenolic facings.

A sandwich structure was modeled as shown in Figure 53.

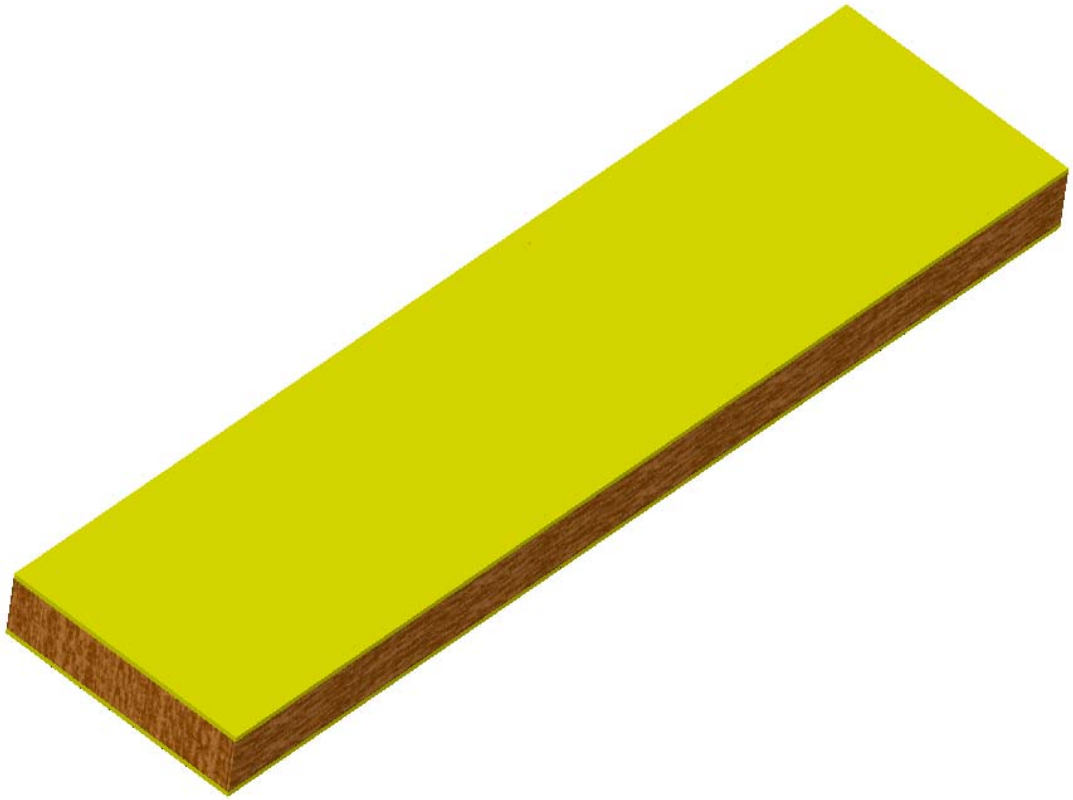

Figure 53: The actual model of sandwich coupon

Boundary conditions were applied on to the sandwich after it was modeled. The following were the boundary conditions applied to the sandwich coupon.

1. Pressure on the bearing plate placed on top of the sandwich composite
2. Setting X-translation free and Y and Z translations as constant for the bottom left edge (along the width).
3. Setting Two bottom left points with X,Y,Z translations as constants and rotations as free.
4. Setting X and Z-translations for right bottom edge (along the width) to free and Y as constant.

Figure 54 shows all the above boundary conditions applied to balsa wood core composite sandwich with glass phenolic facings.

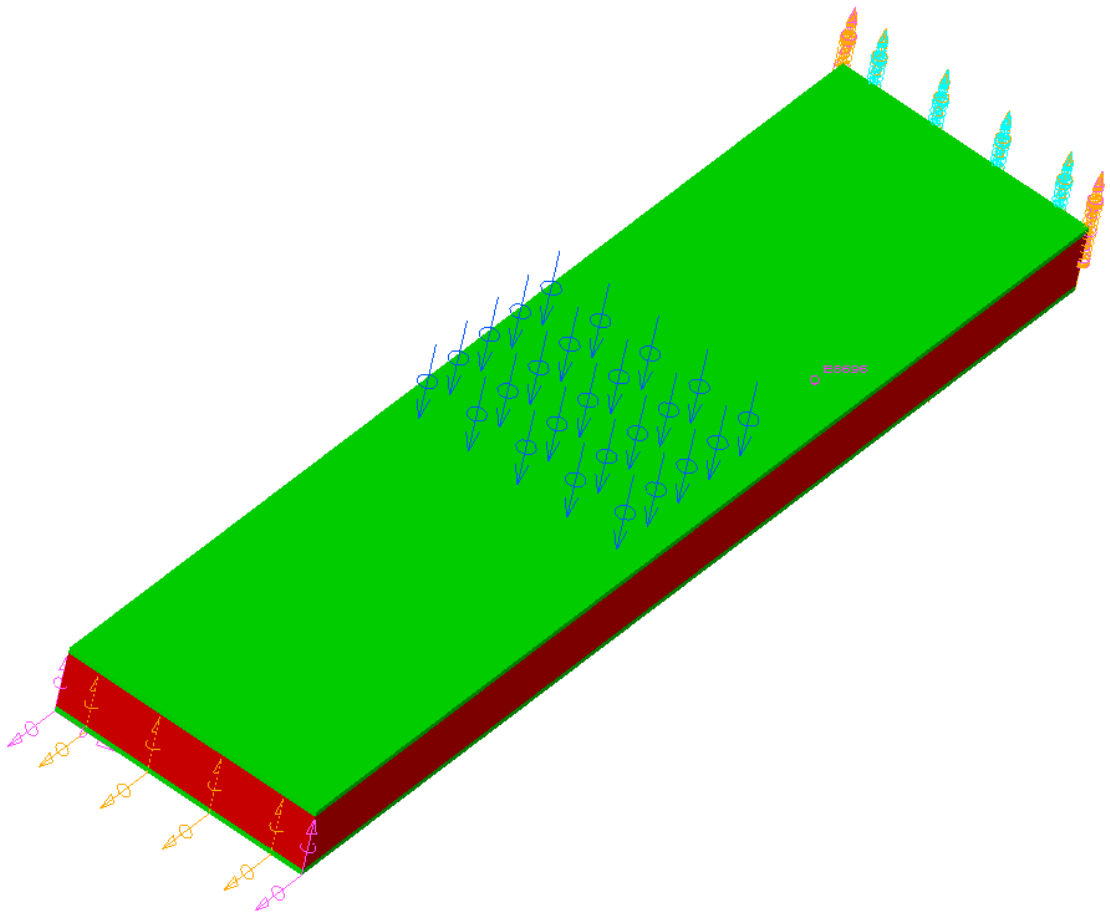

Figure 54: The sandwich coupon with boundary conditions

After the boundary conditions are applied, the sandwich composite is meshed using tetrahedral elements and an element size of 0.01 inches.

After meshing, a load set and a boundary condition set is created and the problem is solved for stresses, strains and deflections.

Figure 55 illustrates a schematic of the sandwich after applying boundary conditions and meshing.

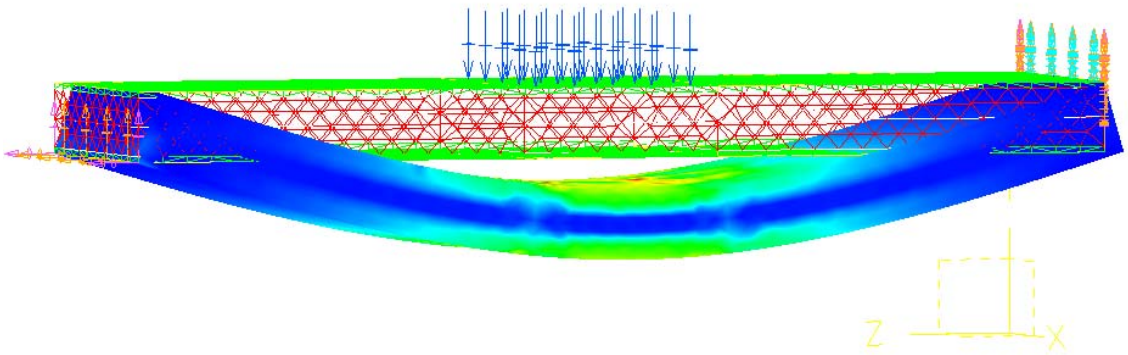

Figure 55: The sandwich coupon after applying boundary conditions and meshing

The boundary condition set and the solution set were created. The model then is ready for solving. The model is then solved and analyzed.

Finite Element Analysis results were compared to results obtained theoretically, as well as, results obtained from the experiments.

Chapter 7: Conclusions

7.1 Balsa wood core composite sandwich with glass fiber polyester facings

Theoretical analysis was done on balsa wood core composite sandwich with glass fiber polyester facings using the flexure formulae for sandwich composites. The analytical results were compared with the actual experimental values and it seems like there is a close connection between these values. The values do not vary by a large difference. The maximum load recorded on the MTS machine for 1 inch thick balsa wood core composite sandwich was 1131.23 pounds and the maximum deflection at the point of maximum load was 0.1833 inches.

7.2 Balsa wood core composite sandwich with glass phenolic facings

The analytical results were compared with the actual experimental values and it seems like there is a close connection between these values. The values do not vary by a large difference. The statistical analysis proves that there is a significant difference between the tests done at room and elevated temperature. The glass transition temperature for glass phenolic is around 220 degrees Celsius. Glass phenolic with good resin curing may have glass transition temperatures around 350 degrees Celsius. However, the material properties like the modulus of elasticity go down after the glass transition temperature because, above this point, a non crystalline phenolic exhibits the properties of a rubbery solid or a viscous liquid. Further, cooling results in the phenolic transforming into a hard, brittle, glass-like material which now has increased stiffness and behaves in a highly elastic fashion.

In this case, there was a difference in the mean failure load for tests done at room and elevated temperature. It was observed that the failure load at elevated temperature was lower than the failure load at room temperature, which means for glass phenolic, the modulus of

elasticity decreases with the increase in temperature and then it suddenly rises at a point and continues to increase until glass transition temperature is reached and then decreases rapidly.

A finite element model was developed using IDEAS software and it was found that the results obtained were also in close connection with theoretical results and experimental values.

The following table shows the length, width, thickness, temperature when tested, failure load and analytical deflection.

Table 4: Summary of sandwich test measurements at elevated temperature

Specimen Geometry (6 cut from each panel)	Length (in)	Width (in)	Thickness (in)	Testing temp (degrees C)	Experimental failure load (lb)	Experimental deflection (in)	Analytical deflection (in)
Dutta -1A	12.00	1.922	0.551	60	191.19	0.150	0.154
Dutta -1B	12.00	1.923	0.550	59	262.00	0.211	0.211
Dutta -1C	12.00	1.925	0.550	61	269.19	0.218	0.216
Dutta -1D	12.00	1.924	0.552	61	172.80	0.130	0.138
Dutta -1E	12.00	1.939	0.559	59	275.27	0.207	0.221
Dutta -1F	12.00	1.936	0.552	61	275.13	0.218	0.221
Dutta -2A	12.00	1.933	0.551	59	258.06	0.216	0.207
Dutta -2B	12.00	1.924	0.551	60	285.89	0.219	0.230
Dutta -2C	12.00	1.934	0.559	59	255.52	0.201	0.205
Dutta -2D	12.00	1.943	0.550	61	269.60	0.212	0.217
Dutta -2E	12.00	1.922	0.551	61	246.80	0.202	0.198
Dutta -2F	12.00	2.052	0.550	61	278.90	0.222	0.223
Dutta -3A	12.00	1.932	0.552	61	241.86	0.193	0.194
Dutta -3B	12.00	1.935	0.551	61	221.30	0.176	0.178
Dutta -3C	12.00	1.921	0.559	61	258.52	0.210	0.208
Dutta -3D	12.00	1.921	0.552	61	219.17	0.180	0.180
Dutta -3E	12.00	1.925	0.559	60	262.69	0.219	0.211
Dutta -3F	12.00	1.948	0.559	60	262.55	0.223	0.211
Dutta -4A	12.00	1.936	0.551	61	247.47	0.197	0.199
Dutta -4B	12.00	1.940	0.551	60	245.23	0.184	0.197
Dutta -4C	12.00	1.925	0.551	60	250.06	0.186	0.201

Dutta -4D	12.00	1.935	0.550	59	248.27	0.191	0.199
Dutta -4E	12.00	1.939	0.550	60	289.74	0.221	0.233
Dutta -4F	12.00	1.925	0.551	62	287.03	0.223	0.231
Dutta -5A	12.00	2.012	0.559	60	291.93	0.238	0.235
Dutta -5B	12.00	1.934	0.550	62	254.21	0.207	0.204
Dutta -5C	12.00	1.922	0.559	60	257.30	0.215	0.207
Dutta -5D	12.00	1.921	0.552	60	232.15	0.188	0.186
Dutta -5E	12.00	1.926	0.551	61	319.50	0.254	0.257
Dutta -5F	12.00	1.922	0.550	60	364.40	0.281	0.290
Dutta -6A	12.00	1,923	0.550	61	270.04	0.207	0.217
Dutta -6B	12.00	1.927	0.557	60	174.24	0.143	0.140
Dutta -6C	12.00	1.925	0.559	61	237.90	0.189	0.191
Dutta -6D	12.00	1.945	0.551	60	258.60	0.213	0.208
Dutta -6E	12.00	1.921	0.551	60	243.40	0.185	0.196
Dutta -6F	12.00	1.932	0.550	61	268.05	0.223	0.215

Table 5: Summary of sandwich test measurements at room temperature

Specimen Geometry (6 cut from each panel)	**Length (in)**	**Width (in)**	**Thickness (in)**	**Exp. Failure Load (lb)**	**Experimental deflection (in)**	**Analytical deflection (in)**
Dutta -7A	12.00	1.921	0.550	311.15	0.223	0.250
Dutta -7B	12.00	1.924	0.552	266.80	0.201	0.214
Dutta -7C	12.00	1.928	0.551	257.25	0.200	0.207
Dutta -7D	12.00	1.924	0.556	313.80	0.223	0.252
Dutta -7E	12.00	1.922	0.559	249.50	0.190	0.200
Dutta -7F	12.00	1.945	0.550	320.05	0.240	0.257
Dutta -8A	12.00		0.550	184.39	0.134	0.148
Dutta -8B	12.00	1.939	0.551	316.14	0.233	0.254
Dutta -8C	12.00	1.936	0.558	322.42	0.240	0.259
Dutta -8D	12.00	1.927	0.553	285.64	0.220	0.230
Dutta -8E	12.00	1.927	0.555	295.64	0.210	0.238
Dutta -8F	12.00	1.956	0.551	330.00	0.234	0.260
Dutta -9A	12.00	1.924	0.550	333.08	0.240	0.268

Dutta -9B	12.00	1.956	0.553	305.14	0.230	0.245
Dutta -9C	12.00	1.924	0.557	328.27	0.243	0.262
Dutta -9D	12.00	1.921	0.552	316.63	0.230	0.255
Dutta -9E	12.00	1.965	0.559	344.51	0.250	0.277
Dutta -9F	12.00	1.922	0.559	324.9	0.240	0.261

For the balsa wood core composite sandwich with glass phenolic coupons, four different failure phenomenons were observed and analyzed. The different types of failures were critical interface failure, core failure, facing plate failure (cracking of the facing plate), and a part of the core sticking to the facing.

Critical interface failure occurred at low loads than normal or average failure load. The failure seems to have occurred because of imperfect bonding between the core and the facing plates. The core failure and the facing plates failure occurred at loads close to the average failure load.

The final failure mechanism, a part of core sticking to the facing plate occurred for coupons which failed at relatively higher loads than normal average failure load. This type of failure occurs when the facing plate is in a yielding mode and on application of more load, ‘plastic hinge’ is formed on the facing plate and the load is transferred to the core which resulted in part of the core sticking to the core when the coupon failed. It was also observed that the failure in this type of failure mechanism came close to the point of contact of the piston and the sandwich coupon.

Some of the failures obtained from the experiments can be eliminated by using the functionary graded materials concept.

7.3 Functionally Graded Materials

A functionally graded composite material (FGM) is two component composite characterized by compositional gradient from one component to the other. The concept of Functionally Graded Materials originated in Japan 1984 for a space plane project. They proposed FGM's as a thermal barrier for withstanding a surface temperature of 2000 K and a temperature gradient of 1000 K across a cross section of less than 10 mm.

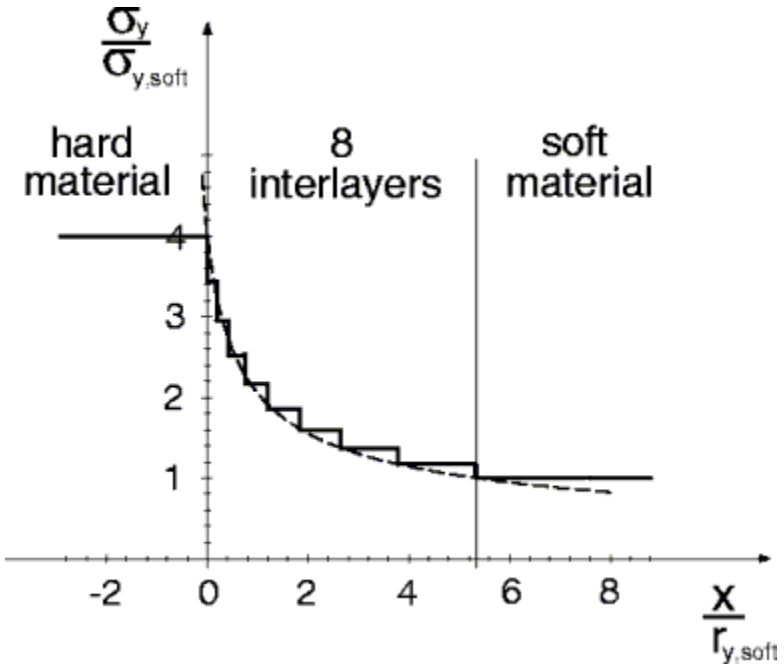

Figure 56: Variation of modulus in FGMs [14]

Functionary Graded Materials have great applications in severe operating conditions. For example wear-resistant linings for handling large heavy abrasive ore particles, rocket heat shields, heat exchanger tubes, thermoelectric generators, heat-engine components, plasma

facings for fusion reactors, and electrically insulating metal/ceramic joints. They are also ideal for minimizing thermo mechanical mismatch in metal-ceramic bonding.

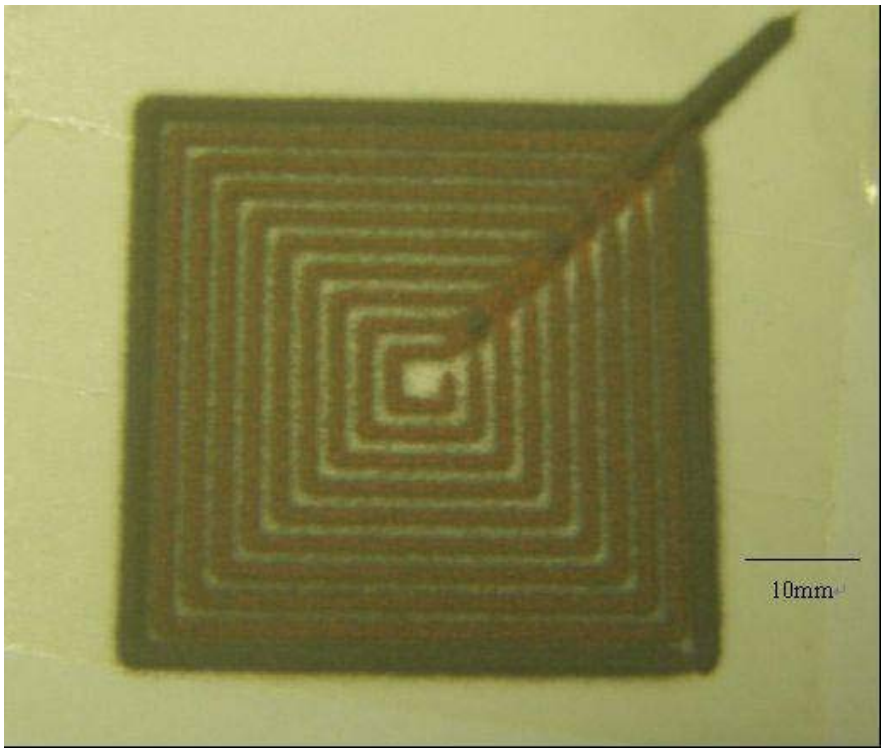

Figure 57: A Functional Gradient, 100% steel at the outside to 30% steel – 70% copper at the center [14]

Bulk FGMs

FGMs with gradient breadth in order of millimeters to centimeters, and with continuous profiles are called Bulk FGMs. These kinds of FGMs are used for the most extreme environment cases.

Water Resistant FGMs

There are FGMs made out of metals and ceramics which have the capability of resisting water. A low–cost ceramic metal functionality with water resistance would be ideal for wear-resistant linings in the mineral processing industry. Such a material would have the following properties:

- High abrasion resistance
- Convenience: can be easily bolted/welded to the metal supports
- High Impact resistance.

References

1. Dr.Dutta and Dr.Hui, Experimental results of shipboard thick composite structures from thermo-mechanical stresses of fire, September 2005
2. .L. Tararielli, N.A. Fleck, V.S.Deshpande, Collapse of clamped and simply supported composite sandwich beams in three-point bending, July 2003 Composites Engineering
3. H. Judawisastra, J. Ivens, and I. Verpoest, Determination of core shear properties of three dimensional woven sandwich composites
4. R.M. Ogorkiewicz and P.E.R.Mucci , Testing of Fibre- Plastic Composites in Three-Point Bending
5. V.Crupi, R.Montanini, Aluminum Foam Sandwiches Collapse Modes under Static and Dynamic Three-Point Bending
6. Nikhil Gupta, Eyassu Woldesenbet, Kishore, S.Sankaran, Response of Syntactic Foam Core Sandwich Structured Composites in Three-Point Bending
7. Jack R Vinson, The Behavior of Sandwich Structures of Isotropic and Composite Materials. Technologic Publishing Co., Inc
8. Robert M Jones, " Mechanics of Composite Materials", Hemisphere Publishing Corporation
9. Dan Zenkert, Introduction to Sandwich Construction, Engineering Materials Advisory Services Limited
10. Charles T Lynch, Handbook of material science, CRC Press
11. Michael F Ashby, Material selection in mechanical design, Butterworth Heinemann
12. Charles E. S. Ueng, Sandwich Composites, Georgia Institute of Technology

13. Allen, H. G, Analysis and design of structural sandwich panels, Pergamom, New York.

14. www.google.com

15. www.composites.about.com

16. http://www.oneoceankayaks.com/Sandcore.htm

17. http://www.aviation-history.com/dehavilland/mosquito.html

18. www.efunda.com

Appendices

1. Setting up the MTS machine

Steps	Key Points/Illustrations
Turn on the water supply to the hydraulic motor	The motor will get overheated without adequate cooling.
Plug the load cell to left connector of module 4	Back panel of Micro Console. There are 2 connectors on module 2.
Disconnect pin 3 and 4. This disables the Micro Profiler. The command signal is now generated from the PC station. Refer to MTC Machine (PC Data Collection).	To disconnect pin 3 and 4, pull out the Micro Profiler module.
Turn on power supply to the Micro Console	Back panel of Micro Console
Hit [Enter] button after the controller has initialized.	
Activate the AC Controller/Displacement Module by pressing the [Display] button on the AC Controller. Green light appears above the [Display] button of the Displacement Module. Select the Traducer Full Scale [Display Select Buttons]. It must the same as the load cell attached to the bottom of the module. Select DC Error by using the [Display Select] buttons on the Micro Console. Set DC Error to zero by tuning the [Set Point] knob on the AC Controller.	The Displacement module is active. The interactive display screen shows the value of the selected parameter of the displacement module. The DC controller is configured for displacement.
Activate the DC Controller/Load Module by pressing the [Display] button on the DC Controller. Green light appears above the [Display] button of the Load Module. Select Transducer Output by using the [Display Select] buttons on the Micro Console. Set transducer output to zero by tuning the [Zero] knob on the DC Controller.	The Force Module is active. The interactive display unit shows the value of the selected parameter of the force module. The AC controller is configured for load.

Set all light indicators on the Micro Console to green color and start the hydraulic motor. First press the [Low] and then [High] buttons on the Micro Console.	Set indicators to green by pressing [Disable/Enable] button.
Go to PC setup. The cursor should be on the [GO]. Hit return key.	You will hear a loud noise. The displacement/time and load/time charts are displayed.
Align the contact surface of the machine ram. Carefully turn the [Zero] knob on the DC Controller unit to bring the ram upward until the surfaces is about/just to contact. Bring the ram down to have ample space to load your sample.	Clockwise- ram moves upward. Anti-clockwise – ram moves downward.
Set up sample. It should be lubricated with high pressure grade grease and Teflon sheets at both ends. This is to ensure no barreling of the sample during compression	
Slowly turn the [Zero] knob on the AC Controller/Displacement Module until the sample touches the top ram.	Use the interactive display screen on the Micro Console to guide you. The reading should remain about zero.
You are now ready. Go back to PC and hit the enter key. Hit the Esc key when completed.	Load and displacement graph should be generated as experiment proceeds. Refer to MTS Machine to save the data.
Bring down the ram by turning the [Zero] knob on the AC Controller/Displacement Module anti-clockwise. Turn off the hydraulic pump in sequence, [Low] and then [Off].	
Turn off the power supply to the Micro Console. Turn off the water supply and remove your sample. Clean up.	

2. Finite Element Analysis pictures

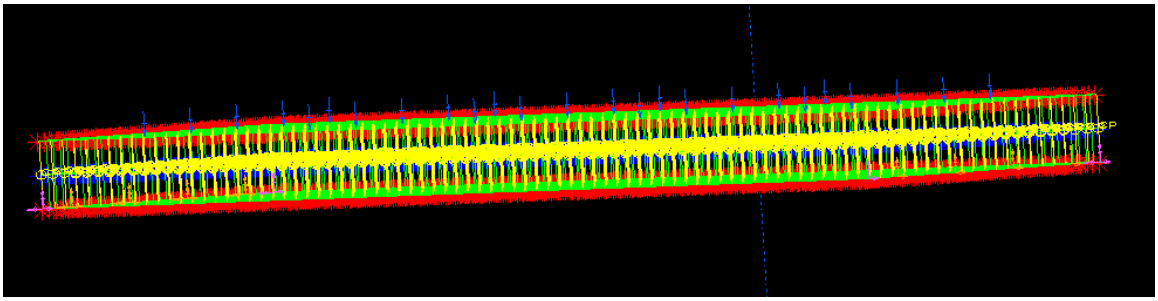

Side view of the balsa wood core sandwich composite

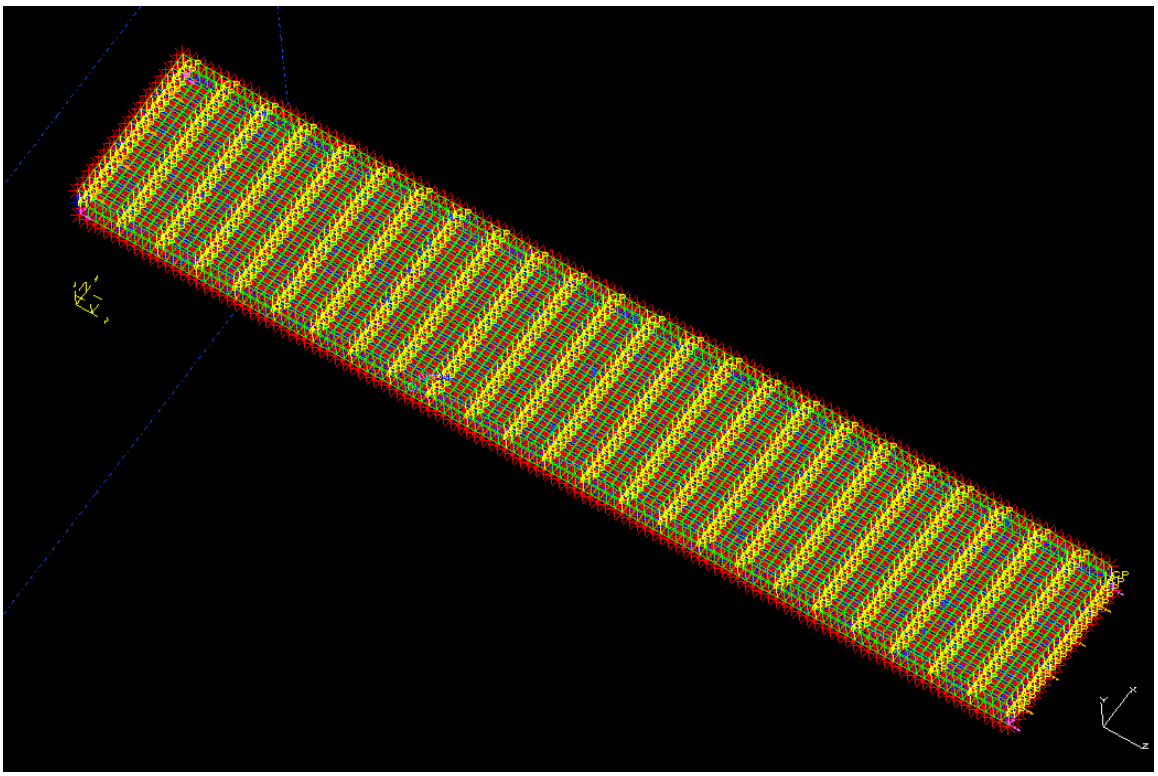

Meshed sandwich coupons with coupled degree of freedom

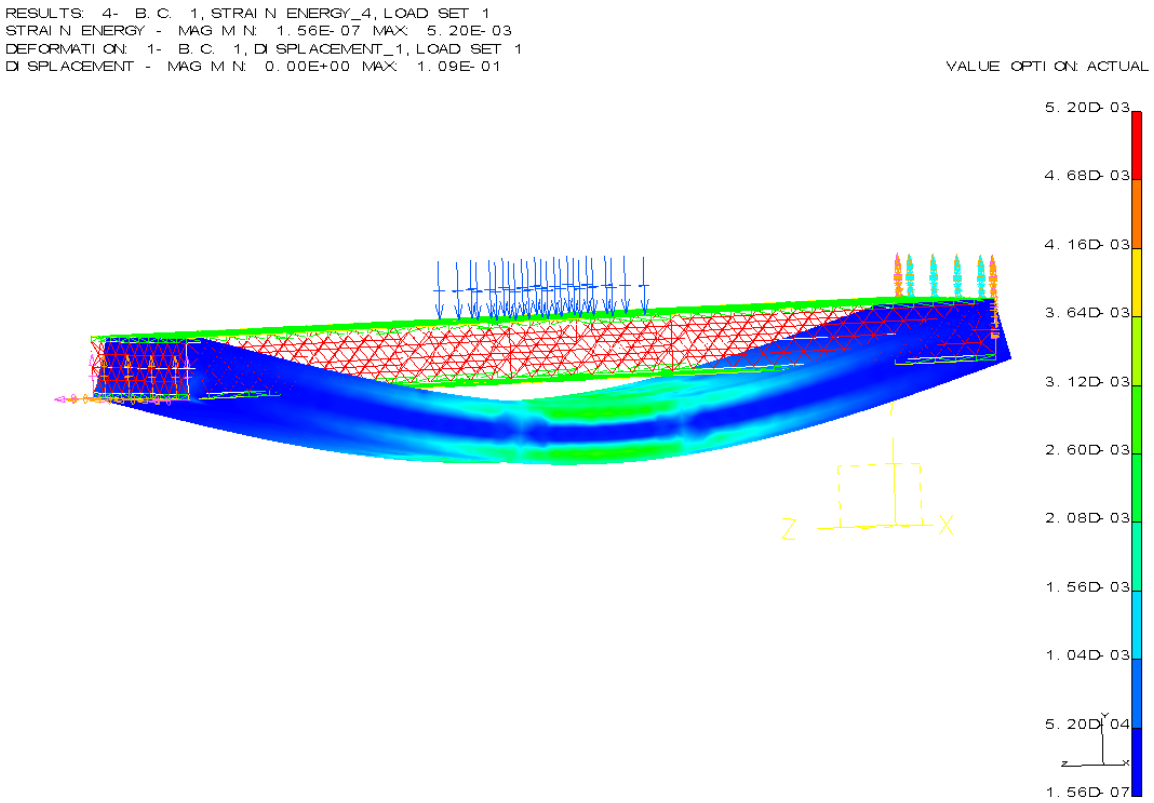

Strain distribution for balsa wood core composite sandwich with glass phenolic facings

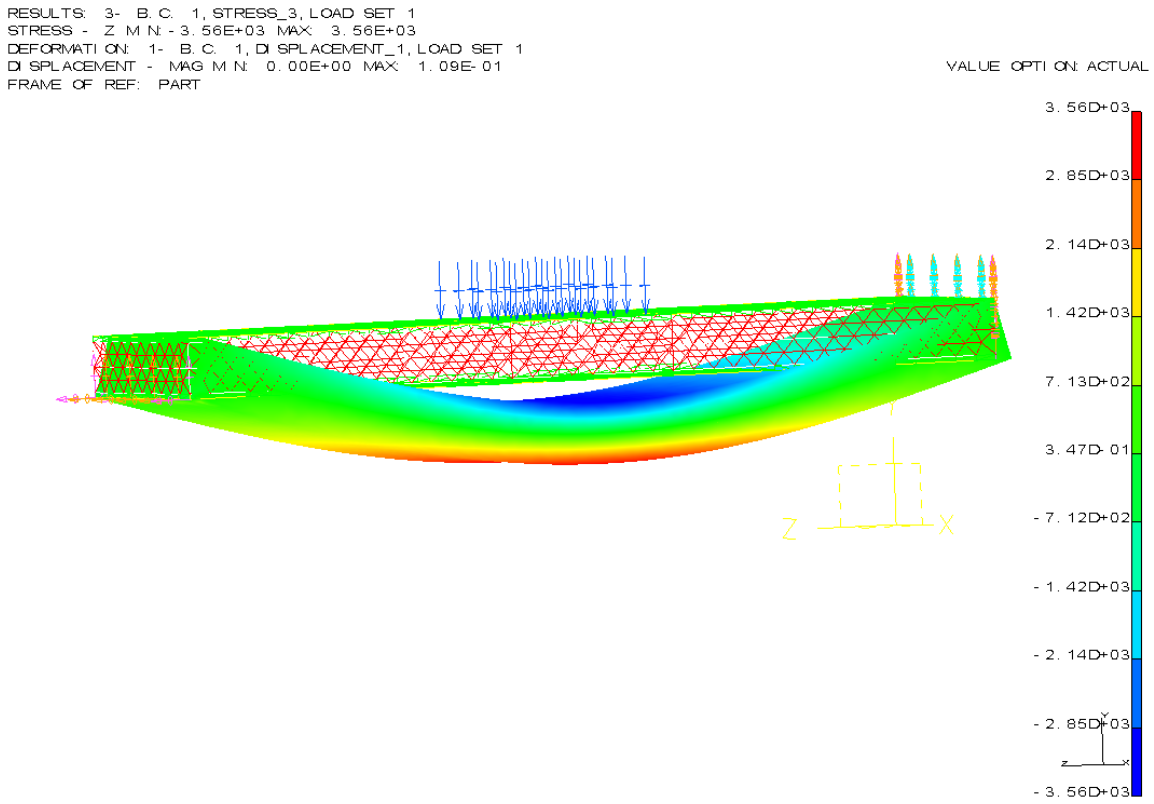

Stress distribution for balsa wood core composite sandwich

Vita

Sandeep Nallagula finished Bachelor of Science from Jawaharlal Nehru Technological University, India. Sandeep is an engineering student with an extensive background in design, manufacturing, heat transfer and in the field of composites.

His background in composites includes experiments like three point bending and four point bending tests to calculate core shear stress, flexural stiffness, average Facing Stiffness and deflection of Balsa Wood Core Composite Sandwich and Aluminum Honeycomb Core Composite Sandwich beams by analytical and computational stress analysis. Tests performed determine the maximum failure load, maximum deflection, percentage strain under the ASTM standards. He also developed a model which is used to find the heat transfer coefficient, temperature and velocity distributions in mini and micro channels. He worked on his thesis "Behavior and Flexure analysis of Sandwich Composite beams" to analyze the Balsa Wood Core Composite Sandwich for different facings like Glass Polyester and Glass Phenolic at different temperatures. His ability to grasp things faster and analyze have contributed to my success in the Mechanical Engineering field.

He worked for a defense company designing and manufacturing "Nozzle Support" with three other guys in his team and they all managed to increase its efficiency by changing its design aspects which proved to be highly productive for the company.

He possesses excellent skills in design, manufacturing and is adept at preparing reports and presentations. He is able to motivate personnel at all levels. In addition, his tact and people skills have helped to make him particularly effective.